Aus der Abteilung für Hand-, Plastische

und Ästhetische Chirurgie

Klinik der Universität München

Direktor: Professor Dr. Riccardo E. Giunta

Neue Anwendungsmöglichkeiten der dreidimensionalen Oberflächenerfassung zum Vergleich der Akuttoxizität radioonkologischer Fraktionierungsschemata beim Mammakarzinom sowie zur Ganzkörperscan-gestützten Verlaufsdokumentation und volumetrischen Evaluation plastisch-chirurgischer Eingriffe der unteren Extremität

Kumulative Dissertation

zum Erwerb des Doktorgrades der Medizin

an der Medizinischen Fakultät der

Ludwig-Maximilians-Universität zu München

vorgelegt von

Lucas Etzel

aus Stuttgart

2023

Mit Genehmigung der Medizinischen Fakultät

der Universität München

Berichterstatter:	Prof. Dr. Riccardo E. Giunta
Mitberichterstatter:	Prof. Dr. Karl-Hans Englmeier
	Prof. Dr. Andrea Baur-Melnyk
Mitbetreuung durch die promovierten Mitarbeiter:	Prof. Dr. Thilo Schenck
	Dr. Konstantin Koban
Dekan:	Prof. Dr. med. Thomas Gudermann
Tag der mündlichen Prüfung:	02.02.2023

Eidesstattliche Versicherung

Ich erkläre hiermit an Eides statt,

dass ich die vorliegende Dissertation mit dem Titel:

„Neue Anwendungsmöglichkeiten der dreidimensionalen Oberflächenerfassung zum Vergleich der Akuttoxizität radioonkologischer Fraktionierungsschemata beim Mammakarzinom sowie zur Ganzkörperscan-gestützten Verlaufsdokumentation und volumetrischen Evaluation plastisch-chirurgischer Eingriffe der unteren Extremität“

selbständig verfasst, mich außer der angegebenen keiner weiteren Hilfsmittel bedient und alle Erkenntnisse, die aus dem Schrifttum ganz oder annähernd übernommen sind, als solche kenntlich gemacht und nach ihrer Herkunft unter Bezeichnung der Fundstelle einzeln nachgewiesen habe.

Ich erkläre des Weiteren, dass die hier vorgelegte Dissertation nicht in gleicher oder in ähnlicher Form bei einer anderen Stelle zur Erlangung eines akademischen Grades eingereicht wurde.

München, 11.02.2023	Lucas Etzel
Ort, Datum	Unterschrift Doktorand

Inhaltsverzeichnis

Abkürzungsverzeichnis

2D – Zweidimensional

3D – Dreidimensional

3DOE – Dreidimensionale Oberflächenerfassung

CF-RT – Konventionell fraktionierte Strahlentherapie

CT – Computertomographie

HF-RT – Hypofraktionierte Strahlentherapie

LMU – Ludwig-Maximilians-Universität München

MRT – Magnetresonanztomographie

PROMs – Patient-Reported Outcome Measures

Publikationsliste der kumulativen Dissertation

Die vorliegende Dissertation umfasst die folgenden in referierten Fachzeitschriften veröffentlichten Originalarbeiten:

Koban, K.C., **Etzel, L.**, Li, Z., Pazos, M., Schönecker, S., Belka, C., Giunta, R.E., Schenck, T.L., Corradini, S.: Three-dimensional surface imaging in breast cancer: A new tool for clinical studies? Radiation Oncology. 15, 1–8 (2020). https://doi.org/10.1186/s13014-020-01499-2

Journal Impact Factor 2020 = 3,481

Clarivate Journal Citation Reports Kategorie RADIOLOGY, NUCLEAR MEDICINE & MEDICAL IMAGING: Journal Impact Factor Rank 2020 = 50/133 (Q2)

Etzel, L., Schenck, T.L., Giunta, R.E., Li, Z., Xu, Y., Koban, K.C.: Digital Leg Volume Quantification: Precision Assessment of a Novel Workflow Based on Single Capture Three-dimensional Whole-Body Surface Imaging. Journal of Digital Imaging. 34, 1171–1182 (2021). https://doi.org/10.1007/s10278-021-00493-8

Journal Impact Factor 2021 = 4,903

Clarivate Journal Citation Reports Kategorie RADIOLOGY, NUCLEAR MEDICINE & MEDICAL IMAGING: Journal Impact Factor Rank 2021 = 36/136 (Q2)

1 Übergeordnete Einleitung

1.1 Dreidimensionale Oberflächenerfassung

Die dreidimensionale Oberflächenerfassung (3DOE) ist eine in der Medizin zunehmend häufig angewandte Bildgebungsmodalität zur präzisen digitalen Erfassung der Geometrie und Textur der Körperoberfläche [1]. Dabei sind die verschiedenen zugrundeliegenden Technologien mit unterschiedlichen Stärken und Limitationen bezüglich der Scan-Auflösung, der Texturerfassung und der Aufnahmegeschwindigkeit assoziiert [2–5].

Eine klinische bewährte Andwendungsform der 3DOE ist die Nahbereichs-Photogrammmetrie [5]. Hier erfolgt die berührungslose Oberflächenerfassung, indem am Computer ein dreidimensionales Modell des Körpers aus multiplen überlappenden zweidimensionalen (2D) Fotografien errechnet wird. Großgeräte mit mehreren integrierten Kameras können durch die synchronisierte Aufnahme im Sekundenbruchteil Bilddatensätze zur Scan-Berechnung generieren [6–9]. Während solche Scanner 3D Aufnahmen frei von Bewegungsartefakten und mit hoher Texturauflösung erfassen können, benötigen sie oft eine Festinstallation [3]. Aus diesem Grund wurden in den letzten Jahren kleinere Geräte auf der Basis einzelner Kameras entwickelt, welche zunehmend die mobile Anwendung zur akkuraten Erfassung des Körpers ermöglichen [10–12].

Im Vergleich dazu funktionieren Strukturlichtscanner durch Projektion eines Lichtmusters auf das abzubildende Körperareal [3, 13]. Da sich das Lichtmuster abhängig von der Geometrie auf der Körperoberfläche verformt, erlaubt der Scanner durch Triangulation dieser Veränderungen die

digitale Rekonstruktion der Körperform im Sinne eines digitalen Datenmodells [3]. In der *Abbildung 1.1* ist eine exemplarische Übersicht eines 3D Strukturlichtscans der weiblichen Brust dargestellt.

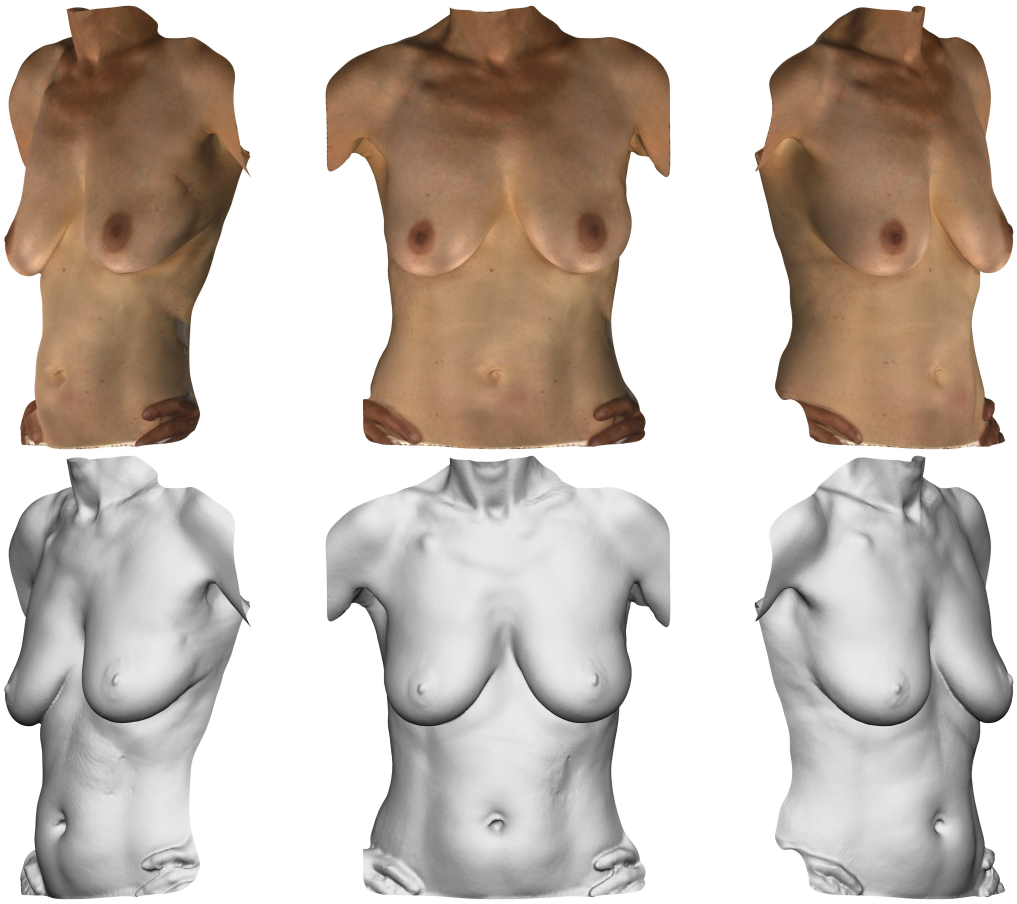

Abbildung 1.1: Texturierte und untexturierte Übersicht eines 3D Strukturlichtscans der weiblichen Brust am Beispiel einer 50-jährigen Patientin mit linksseitigem Mammakarzinom.

Diese Scanner erlauben eine sehr präzise Erfassung der Geometrie, und sind vergleichend zu photogrammetrischen Scannern robuster bei der Erfassung behaarter Körperareale [14]. Da es sich oft um kompakte handgeführte Scannermodelle handelt, erlauben entsprechend

leistungsstarke Geräte eine flexible und mobile Anwendung der Bildgebungstechnologie [7, 14]. Durch Miterfassung texturierter Einzelbilder erlaubt diese Form der 3DOE ebenfalls eine Texturierung der hochauflösenden 3D Aufnahmen [15].

Insgesamt ermöglichen die beschriebenen Technologien beim klinischen Einsatz eine Digitalisierung und Visualisierung des klinischen Ausgangsbefunds sowie nachfolgenden therapiebedingten morphologischen Veränderungen. Somit können sie als Instrument zur klinischen Verlaufsdokumentation eingesetzt werden. Weiter erlaubt die 3DOE die quantitative Evaluation der Körpermorphologie durch Berechnung von Längen, Winkeln, Flächen und Volumina oder durch eine chromatische Analyse der Oberflächentextur.

In der Literatur ist der Einsatz der 3DOE in der klinischen Praxis verschiedener Fachrichtungen fest etabliert: So stellt die 3DOE in der plastischen Chirurgie eine etablierte Methode zur objektiven Beurteilung morphologischer Veränderungen der weiblichen Brust dar [8, 16–22]. Weiter kann hier mit medizinischer Software der Einsatz von Implantaten zur Planung einer Mammaaugmentationsplastik simuliert werden [16, 23]. Außerdem finden sich in der Literatur immer neue Anwendungsmöglichkeiten der 3DOE, beispielsweise in der Viszeralchirurgie zur Dokumentation bariatrischer Eingriffe [24], in der Pädiatrie zur Dokumentation vaskulärer Malformationen [25], in der Mund-Kiefer Gesichtschirurgie zur digitalen Registrierung des Gebisses mit dem extraoralem Weichgewebe [26], sowie in der Protethik zur morphologischen Evaluation bei der Stumpfversorgung [27].

Im Gegensatz zu anderen Bildgebungsmodalitäten wie der Computertomographie (CT) oder der Magnetresonanztomographie (MRT) zeichnet sich die 3DOE als strahlenfreie, günstigere und schnellere Aufnahmemethode aus [4, 28].

1.2 Eingesetzte 3D Scanner und Auswertungssoftware

Die 3DOE erfolgte in den vorliegenden Originalarbeiten mit mobilen handgeführten Strukturlichtscannern. In der ersten Publikation wurde der Artec Eva Scanner (Artec 3D, Luxemburg) zur digitalen Erfassung der weiblichen Brust im Rahmen der radioonkologischen Therapie beim Mammakarzinom verwendet. Das Aufnahmegerät ist in zahlreichen Validierungsstudien in der Literatur vorbeschrieben und findet in der klinischen Praxis regelmäßige Anwendung zur 3D Dokumentation und digitalen Evaluation der Körpermorphologie [7, 8, 14, 20, 27, 29–34]. Der mobile Scanner wird auch erfolgreich zur intraoperative Anwendung [7] oder im Rahmen anatomischer Studien [29, 31, 35] eingesetzt. Als kompakter 3D Scanner ist für den mobilen Betrieb lediglich die kabelgebundene Verbindung mit einem leistungsstarken Laptop zur Stromversorgung und Datenaufzeichnung erforderlich, weitere Gerätschaften werden für den laufenden Betrieb nicht benötigt. Die scannerspezifische Software Artec Studio (Artec 3D, Luxemburg) ermöglicht dem Anwender eine individuell anpassbare Prozessierung der aufgezeichneten Aufnahmen und erlaubt eine hochauflösende texturierte Rekonstruktion und Analyse der finalen 3D Aufnahmen. Der in *Abbildung 1.2* dargestellte handgeführte 3D Scanner ermöglicht so innerhalb etwa einer halben Minute die präzise und farblich akkurate 3DOE des Brustbereichs.

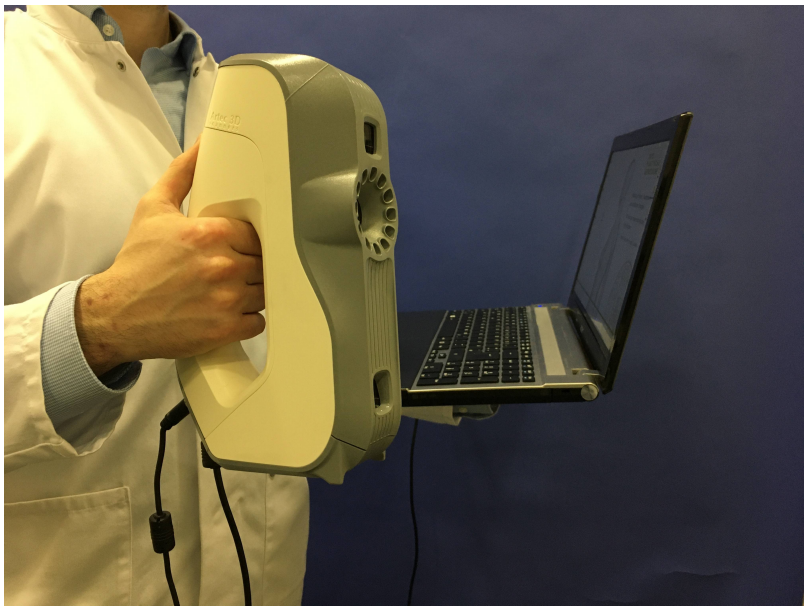

Abbildung 1.2: In Publikation 1 erprobter Artec Eva Strukturlicht 3D Scanner. Abbildung aus Koban, K.C. et al. Three-dimensional surface imaging in breast cancer: a new tool for clinical studies? Radiation Oncology (https://doi.org/10.1186/s13014-020-01499-2) lizensiert unter Creative Commons Attribution 4.0 (http://creativecommons.org/licenses/by/4.0/).

In der zweiten Publikation wurde der Thor3D Scanner (Thor3D, Russland) zusammen mit dem zugehörigen elektrischen Drehtisch (Thor3D, Russland) zur 3D Ganzkörpererfassung und damit zur körpermorphologischen Verlaufsdokumenation verwendet. Das Aufnahmegerät zeichnet sich durch einen integrierten Akku sowie einem größerem Sichtfeld als beim Artec Eva Scanner aus. So ermöglicht der Thor3D Scanner eine komfortable und schnelle Erfassung großer Zielvolumina. Aufgrund dieser Eigenschaften kann der Scanner durch kranio-kaudale Erweiterung der Aufnahmetechnik gemeinsam mit dem elektrischen Drehtisch innerhalb einer Minute zur zuverlässigen Erfassung der Körper-Zirkumferenz und damit zur Digitalisierung nahezu der gesamten Körperoberfläche angewandt werden. Dieses mobile Aufnahmesystem und der Verlauf

der Scanprozessierung zum texturierten Ganzkörperscan ist exemplarisch in *Abbildung 1.3* dargestellt.

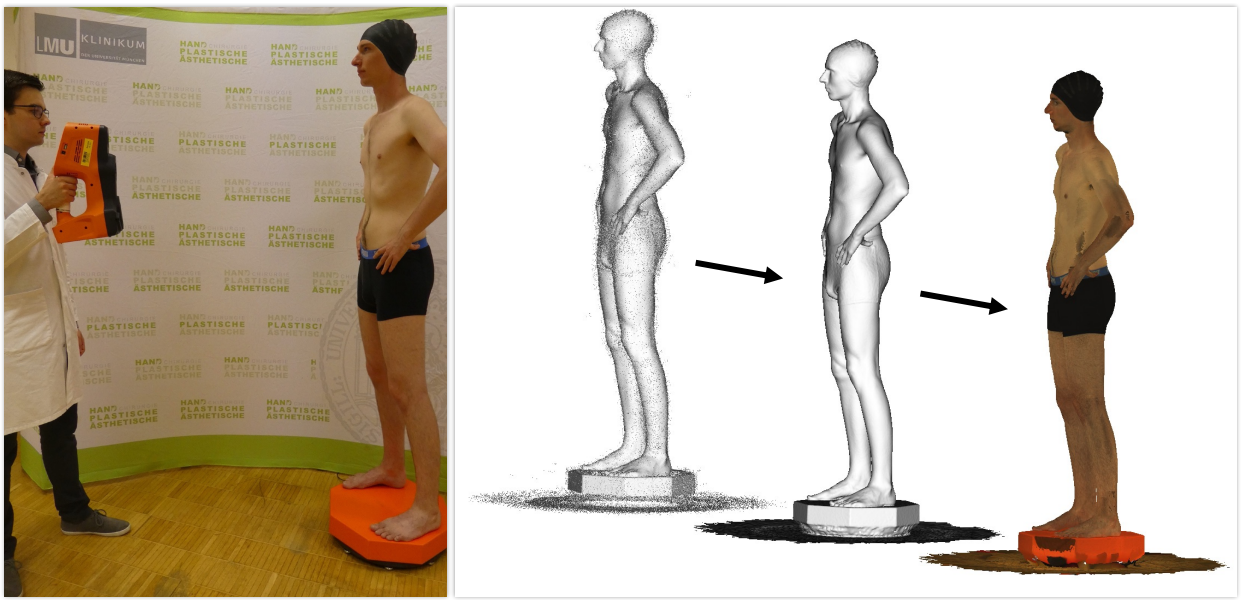

Abbildung 1.3: Beispielhafter Aufbau zur 3D Ganzkörperaufnahme mit dem mobilen Thor3D Scanner und elektrischem Drehtisch sowie Verlauf der Scanprozessierung vom erfassten 3D Datensatz zum untexturierten und texturierten Ganzkörperscan

Als Vorteil gegenüber dem Artec Eva Scanner findet sich bei diesem Gerät ein eingebauter Computer mit Speicherkapazität zur 3D Erfassung ohne Notwendigkeit eines kabelgebundenen separaten Computers zur Aufnahme und Zwischenspeicherung der 3D Aufnahmen. Mit USB-Stick lassen sich die akquirierten Daten auf einen Computer zur Scan-Prozessierung und Analyse übertragen.

Zur weiteren Datenprozessierung und Ausrichtung sowie zum Zuschneiden der 3D Aufnahmen wurden die Aufnahmen im Rahmen der jeweiligen Publikation in der Artec Studio bzw. der

Thor3D Software (Thor3D, Russland) sowie der Geomagic 2010 Software (3D Systems, USA) an einem leistungsstarken Auswertungs-Computer bearbeitet. Die resultierenden 3D Datensätze wurden daraufhin zur Evaluierung und Quantifizierung sowie der Generierung hochqualitativer Grafiken in einer lokale Datenbank der Canfield Mirror Software (Canfield Scientific, Inc., USA) abgespeichert.

1.3 Zielsetzung der kumulativen Dissertation

Das übergeordnete Ziel dieser kumulativen Disseration war es, neue Anwendungsmöglichkeiten der 3DOE zur klinischen Befunddokumentation zu etablieren, und diese hinsichtlich der 3D Quantifizierung der Körpermorphologie zu validieren. Weiter sollte der Mehrwert neuer Anwendungsmöglichkeiten der 3DOE als objektives Instrument zur digitalen Verlaufsdokumentation und Evaluation der Körpermorphologie untersucht werden.

Dazu wurde in einer ersten Publikation die in der plastisch-chirurgischen Routine bereits gängige 3D Evaluation der weiblichen Brust [8, 16–21, 36] in die radioonkologische Praxis zur Verlaufsdokumentation während der adjuvanten Strahlentherapie beim Mammakarzinom übertragen. Während die 3DOE im Rahmen der “Surface-guided Radiation Therapy” [37–40] bereits in der Strahlentherapie zur Lagekontrolle zwischen den Bestrahlungsfraktionen angewandt wird, findet die Technologie bislang keine Anwendung zur Beurteilung von radiogen bedingten Veränderung der Körpermorphologie.

Eine regelmäßige 3D Erfassung der Brust im Rahmen der radioonkologischen Therapie und der klinischen Nachsorge könnte genutzt werden, um als objektives Instrument das Ausmaß akuttoxischer Wirkungen [41–44] wie die beispielhaft in *Abbildung 1.4* dargestellte Radiodermatitis abzubilden.

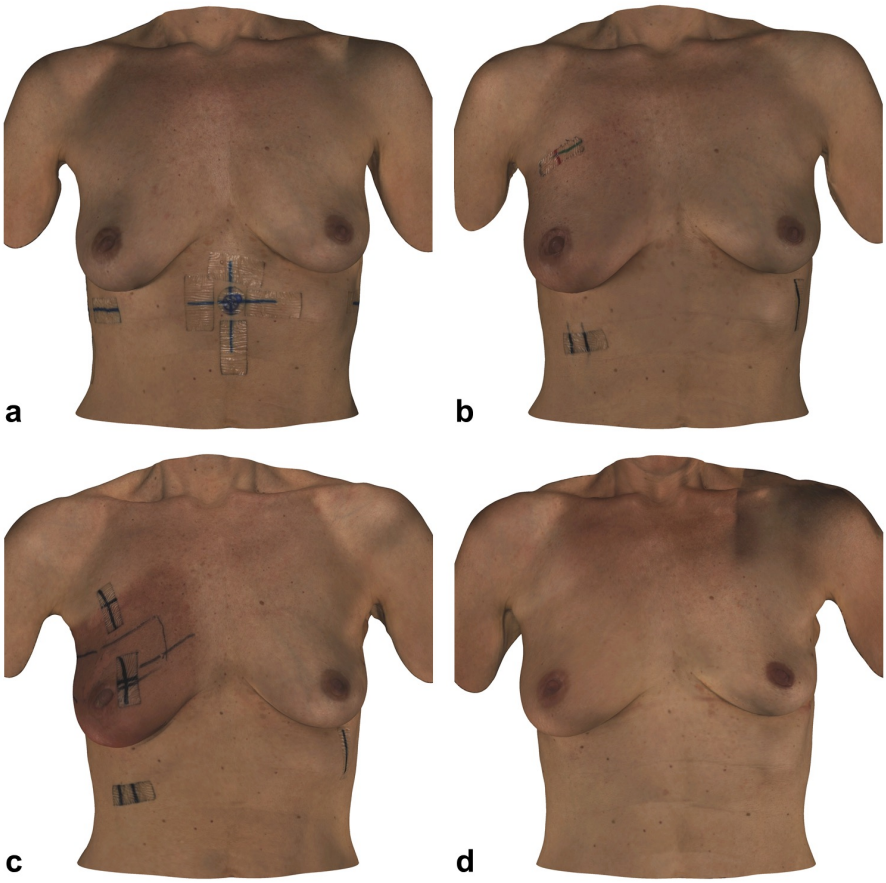

Abbildung 1.4: Verlaufsaufnahmen am Tag der ersten Strahlentherapie (a) sowie nach 3 (b) und 6 (c) Wochen und im Rahmen der klinischen Nachsorge (d) mit unterschiedlichen Ausprägungen einer Radiodermatits der rechten Mamma. Abbildung modifiziert aus Koban, K.C. et al. Three-dimensional surface imaging in breast cancer: a new tool for clinical studies? Radiation Oncology (https://doi.org/10.1186/s13014-020-01499-2) lizensiert unter Creative Commons Attribution 4.0 (http://creativecommons.org/licenses/by/4.0/).

Weiter könnten Auswirkungen wie Schwellung, Hyperpigmentierung und Teleangiektasien objektiv dokumentiert werden. Damit könnte man einen Vergleich zwischen verschiedenen radioonkologischen Fraktionierungsschemata hinsichtlich des ästhetischen Ergebnisses und des Nebenwirkungsprofils durchführen. So untersuchten wir in der ersten Origianlarbeit den neuartigen Einsatz der 3DOE zum Vergleich der Akuttoxizität zwischen der konventionell fraktionierten (CF-RT) und der hypofraktionierten Strahlentherapie (HF-RT) beim Mammakarzinom und evaluierten den Mehrwert zur objektiven Beurteilung von Haut- und Volumenveränderungen der Brust.

Darüber hinaus wollten wir die Erweiterung von anatomisch lokalisierten Scans auf eine Erfassung der Körper-Zirkumferenz zur 3D Ganzkörpererfassung [14, 45, 45–52] erproben. Außerdem wollten wir Arbeitsabläufe zur reproduzierbaren Quantifizierung der akquirierten 3D Datensätze untersuchen. Mithilfe neuer leistungsstarker Scanner wäre eine weitere Beschleunigung und Vereinfachung solcher 3D Akquisen und der zu dokumentierenden und quantitativ analysierbaren Datengrundlange denkbar. Schließlich könnten so mittels standardisierter Aufnahmetechnik die Erfassung schwierig einsehbarer Körperareale wie die Oberschenkel-Innenseiten verbessert werden.

Dazu etablierten wir in einer zweiten Orginalarbeit ein Verfahren zur standardisierten 3D Ganzkörperaufnahme, sowie einen Software-Algorithmus zur Ganzkörperscan-gestützten beinvolumetrischen Quantifizierung. Bislang werden Beinvolumina mit zahlreichen verschiedenen Techniken im klinischen Alltag gemessen [14, 30, 53–61]. So validierten wir unseren Algorithmus hinsichtlich der Wiederholpräzision [62–64] und evaluierten dessen

Anwendung zur Beurteilung plastisch-chirurgischer Eingriffe der unteren Extremität. In *Abbildung 1.5* ist der präzise Vergleich beider Beinvolumina im Rahmen einer einseitigen volumetrisch veränderten Beinmorphologie beim Lymphödem zum Ausganspunkt vor einer mikrochirurgischen Rekonstruktion des Lymphabflusses dargestellt.

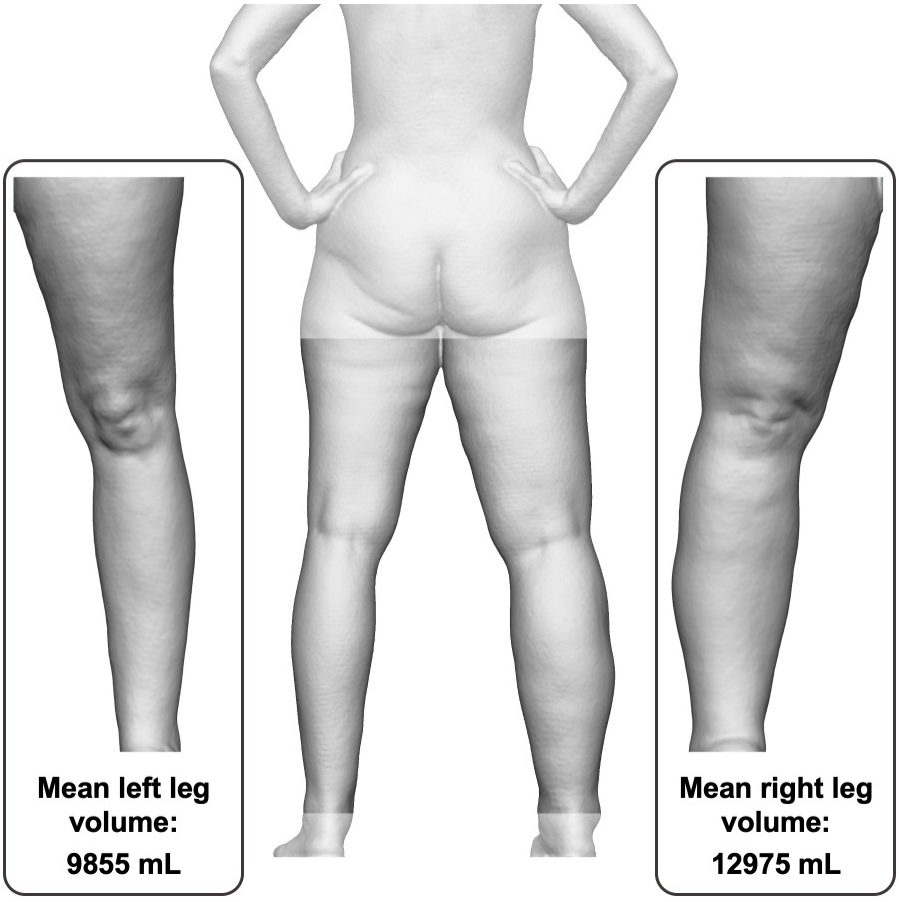

Abbildung 1.5: 3D Ganzkörperscan-gestützter Vergleich der Beinvolumina einer 54-jährigen Patientin mit rechtsseitigem Lymphödem. Abbildung aus Etzel, L. et al. Digital Leg Volume Quantification: Precision Assessment of a Novel Workflow Based on Single Capture Three-dimensional Whole-Body Surface Imaging. Journal of Digital Imaging (https://doi.org/10.1007/s10278-021-00493-8) lizensiert unter Creative Commons Attribution 4.0 (http://creativecommons.org/licenses/by/4.0/).

2 Eigenanteile an den Originalarbeiten

In der Publikation “Three-dimensional surface imaging in breast cancer: a new tool for clinical studies?” beteiligte ich mich als Ko-Autor unter der Supervision von Herrn Dr. Koban und Frau PD Dr. Corradini an der Konzeption der Datenakquise und des Arbeitsablaufs zur 3D Prozessierung und Evaluation. Weiter war ich im Rahmen der radioonkologischen Therapie mit an der Probandenakquise und an der 3D Oberflächenerfassung beteiligt. Anschließend an die 3D Erfassung assistierte ich Dr. Koban bei der 3D Prozessierung und Evaluation. Weiter beteiligte ich mich an der statistischen Auswertung, der Verfassung des Manuskripts und arbeitete unter der Supervision von Dr. Koban die Kommentare der Ko-Autoren ein und fertigte die Manuskript-Abbildungen an.

In der Publikation “Digital Leg Volume Quantification: Precision Assessment of a Novel Workflow Based on Single Capture Three-dimensional Whole-Body Surface Imaging.” konzipierte ich als Erst-Autor nach meiner Literaturrecherche in Zusammenarbeit mit Dr. Koban die Forschungsziele und definierte den Arbeitsablauf für die standardisierte 3D Ganzkörpererfassung. Ich entwickelte eigens den Software-Algorithmus zur Scan-Prozessierung und beinvolumetrischen Quantifizierung. Weiter akquirierte ich gemeinsam mit den Ko-Autoren die Probanden und war maßgeblich für die Durchführung der 3D Ganzkörperfassung verantwortlich. Nach meiner Prozessierung und volumetrischen Auswertung aller 3D Aufnahmen generierte ich mithilfe von selbst programmierten R Skripten alle statistischen Analysen und Graphen. Außerdem verfasste ich eigenständig das Manuskript und erstellte mit der Mirror Imaging Software die 3D Abbildungen zur Veranschaulichung der Methodik und Ergebnisse. Nach Sichtung des

Manuskripts durch meine Ko-Autoren arbeitete ich alle Kommentare ein und wählte das Fachjournal zum Einreichen des Manuskripts aus. Während des Begutachtungsprozesses beantwortete ich die Gutachterfragen und revidierte das Manuskript entsprechend den genannten Verbesserungsvorschlägen. Schließlich war ich bis zur finalen Publikation für die Korrespondenz mit dem Redaktionsbüro des Fachjournals verantwortlich.

3 Zusammenfassung in deutscher Sprache

Ziel dieser Dissertation war die Evaluation des Mehrwerts neuer Anwendungsmöglichkeiten der dreidimensionalen Oberflächenerfassung zur Verbesserung der digitalen Befunddokumentation und der objektiven klinischen Bewertung der Körpermorphologie.

In einer ersten Publikation wurde die in der plastisch-chirurgischen Routine bereits gängige 3D Evaluation der weiblichen Brust [8, 16–21, 36] in die radioonkologische Praxis zur Verlaufsdokumentation während der adjuvanten Strahlentherapie beim Mammakarzinom übertragen. Mithilfe des mobilen Artec Eva Strukturlicht-Oberflächenscanners erfolgte dazu bei 38 Patientinnen wöchentlich während der Therapie sowie bei der ersten klinischen Nachsorge die standardisierte 3DOE der behandelten Brust sowie der kontralateralen gesunden Seite. Die Patientinnen erhielten entweder eine konventionell fraktionierte Strahlentherapie in 25 Fraktionen oder eine hypofraktionierte Strahlentherapie in 15 Fraktionen. Anhand von insgesamt 214 Datensätzen wurden die radiogen bedingten akuttoxischen Auswirkungen der beiden Fraktionierungsschemata verglichen. So zeigten sich im Rahmen der 3D Evaluation hinsichtlich des Brustvolumens im Therapieverlauf in beiden Subgruppen statistisch signifikante Volumenzunahmen der behandelten Brust, wohingegen sich bei der gesunden Brust keine signifikanten Volumenveränderungen zeigten. Weiter konnte in der vorliegenden Publikation das in der Literatur vorbeschriebene seltenere Auftreten von radiogen bedingten Brusterythemen während der HF-RT vergleichend mit der CF-RT [65, 66] bestätigt werden. Somit erlaubt die regelmäßige 3D Erfassung der weiblichen Brust im Rahmen der radioonkologischen Therapie beim Mammakarzinom einen objektiven Vergleich der unterschiedlichen Therapiemodalitäten.

Die beschriebene neuartige Anwendung der 3DOE ermöglicht den quantitativen Vergleich der Akuttoxizität radioonkologischer Fraktionierungsschemata und bietet weiter das Potenzial, objektive 3D Daten im Rahmen klinischer Studien den subjektiven Daten von „Patient-Reported Outcome Measures“ (PROMs) [67] gegenüberzustellen.

In einer zweiten Publikation wurde auf der Basis des mobilen Thor3D Oberflächenscanners und zugehörigem Drehtisch die bereits gängige auf einzelne Körperregionen limitierte 3DOE zu einer standardisierten Aufnahme der nahezu gesamten Körperoberfläche ausgeweitet und an 82 Probanden erprobt. Zusätzlich wurde ein eigens entwickelter Software-Algorithmus zur beinvolumetrischen Quantifizierung hinsichtlich der Präzision validiert und bezüglich der Anwendung zur 3D Dokumentation plastisch-chirurgischer Eingriffe der unteren Extremität evaluiert. Die dargestellte 3D Ganzkörperscan-gestützte Methodik erlaubte dabei unabhängig von der Beinmorphologie eine präzise beinvolumetrische Quantifizierung. Die klinische Anwendung eines solchen Verfahrens ermöglicht den objektiven Vergleich plastisch-chirurgischer Eingriffe der unteren Extremität und kann zur Beurteilung des Befundverlaufs und Therapieerfolgs verschiedener medizinischer Diagnosen und Eingriffe angewandt werden. Dazu zählt beispielweise der Einsatz beim Lymphödem nach onkologischer Resektion oder beim Lipödem, sowie bei den entsprechenden operativen Therapieansätzen wie der mikrochirurgischen Rekonstruktion oder der Liposuktion [14]. Zusätzlich beschleunigt die Akquise standardisierter 3D Ganzkörperaufnahmen und die Etablierung präziser Auswertungsalgorithmen die klinische Anwendung einer 3D-gestützten Befunddokumentation. Außerdem lassen sich so morphologische Veränderungen in mehreren Bereichen des Körpers aufzeichnen, ohne dass die jeweiligen anatomischen Regionen separat erfasst werden müssen.

Zusammenfassend erbringen neue Anwendungsmöglichkeiten der 3DOE eine Verbesserung der digitalen Erfassung und klinischen Evaluation der Körpermorphologie. So ermöglichen die in den vorliegenden Originalarbeiten beschriebenen Einsatzformen der Bildgebungsmodalität die anschauliche Demonstration und präzise Quantifizierung des Befundverlaufs bei radioonkologischen und plastisch-chirurgischen Fragestellungen. Weiter erlauben sie den objektiven Vergleich verschiedener Therapiemodalitäten hinsichtlich des Ergebnisses sowie potenzieller Nebenwirkungen. Die 3DOE könnte somit in Zukunft einen wertvollen Beitrag zur voranschreitenden Digitalisierung bei der Verlaufsdokumentation im medizinischen Alltag leisten. Außerdem kann die Nutzung der Technologie im Rahmen klinischer Studien einen Mehrwert zur evidenzbasierten Medizin liefern.

4 Zusammenfassung in englischer Sprache

The aim of this thesis was to evaluate the added value of new applications of three-dimensional surface imaging to improve the digital documentation of findings and the objective clinical assessment of body morphology.

In a first publication, the 3D evaluation of the female breast [8, 16–21, 36], already commonly used in plastic surgical routine, was transferred to radiooncological practice for documentation during adjuvant radiotherapy for breast cancer. Using the mobile Artec Eva structured light surface scanner, 38 patients underwent standardized 3DOE of the treated breast and the contralateral healthy side weekly during radiotherapy and at the first clinical follow-up. Patients received either CF-RT in 25 fractions or HF-RT in 15 fractions. A total of 214 data sets were used to compare the radiogenic acute toxic effects of the two fractionation regimens. Thus, the 3D evaluation showed statistically significant breast volume increases in the treated breast in both subgroups during the course of therapy, whereas no significant volume changes were seen in the healthy breast. Furthermore, in the present publication, the less frequent occurrence of radiogenic breast erythema during HF-RT, as previously described in the literature, could be confirmed comparatively with CF-RT [65, 66]. Thus, regular 3D acquisition of the female breast during the radiooncological treatment of breast carcinoma allows an objective comparison of the different therapeutic modalities. The described novel application of 3DOE allows for a quantitative comparison of acute toxicity of radiooncologic fractionation regimens and further offers the potential to compare objective 3D data with subjective data from „Patient-Reported Outcome Measures“ (PROMs) [67] during clinical trials.

In a second publication, using the mobile Thor3D surface scanner and associated turntable, the 3DOE, which is commonly limited to individual body regions, was extended to a standardized capture of almost the entire body surface and tested on 82 subjects. In addition, a specially developed software algorithm for volumetric leg quantification was validated for precision and evaluated with regard to its application for 3D documentation of plastic surgery procedures of the lower extremity. The presented 3D whole-body scan-based methodology allowed precise leg volumetric quantification independent of leg morphology. The clinical application of such a method allows an objective comparison of plastically forming procedures of the lower extremity and can be used to evaluate the course of findings and therapeutic success of various medical diagnoses and interventions. This includes, for example, the use in lymphedema after oncological resection or in lipedema, as well as in the corresponding surgical therapy approaches such as microsurgical reconstruction or liposuction [14]. In addition, the acquisition of standardized 3D whole-body images and the establishment of precise evaluation algorithms accelerates the clinical application of 3D-based documentation of findings. It also allows recording of morphological changes in multiple areas of the body without the need to separately capture the respective anatomical regions.

In summary, new applications of 3DOE yield improvements in the digital capture and clinical evaluation of body morphology. For example, the applications of the imaging modality described in the original articles allow for the clear demonstration and precise quantification of the progression of findings in radiation oncology and plastic surgery. Furthermore, they allow the objective comparison of different therapy modalities with regard to outcome as well as potential side effects. In the future, 3DOE could thus make a valuable contribution to the advancing

digitalization in the documentation of progress in everyday medical practice. In addition, the use of the technology in the context of clinical studies can provide added value to evidence-based medicine.

5 Originalarbeiten

5.1 Publikation 1

Koban, K.C., **Etzel, L.**, Li, Z., Pazos, M., Schönecker, S., Belka, C., Giunta, R.E., Schenck, T.L., Corradini, S.: Three-dimensional surface imaging in breast cancer: A new tool for clinical studies? Radiation Oncology. 15, 1–8 (2020). https://doi.org/10.1186/s13014-020-01499-2

Koban et al. Radiation Oncology (2020) 15:52
https://doi.org/10.1186/s13014-020-01499-2

Radiation Oncology

RESEARCH Open Access

Three-dimensional surface imaging in breast cancer: a new tool for clinical studies?

Konstantin Christoph Koban[1*], Lucas Etzel[1], Zhouxiao Li[1], Montserrat Pazos[2], Stephan Schönecker[2], Claus Belka[2], Riccardo Enzo Giunta[1], Thilo Ludwig Schenck[1] and Stefanie Corradini[2]

Abstract

Background: Three-dimensional Surface Imaging (3DSI) is a well-established method to objectively monitor morphological changes in the female breast in the field of plastic surgery. In contrast, in radiation oncology we are still missing effective tools, which can objectively and reproducibly assess and document adverse events in breast cancer radiotherapy within the framework of clinical studies. The aim of the present study was to apply structured-light technology as a non-invasive and objective approach for the documentation of cosmetic outcome and early effects of breast radiotherapy as a proof of principle.

Methods: Weekly 3DSI images of patients receiving either conventionally fractionated radiation treatment (CF-RT) or hypofractionated radiation treatment (HF-RT) were acquired during the radiotherapy treatment and clinical follow-up. The portable Artec Eva scanner (Artec 3D Inc., Luxembourg) recorded 3D surface images for the analysis of breast volumes and changes in skin appearance. Statistical analysis compared the impact of the two different fractionation regimens and the differences between the treated and the contralateral healthy breast.

Results: Overall, 38 patients and a total of 214 breast imaging sessions were analysed. Patients receiving CF-RT showed a significantly higher frequency of breast erythema compared to HF-RT (93.3% versus 34.8%, $p = 0.003$) during all observed imaging sessions. Moreover, we found a statistically significant ($p < 0.05$) volumetric increase of the treated breast of the entire cohort between baseline (379 ± 196 mL) and follow-up imaging at 3 months (437 ± 224 mL), as well as from week 3 of radiotherapy (391 ± 198 mL) to follow-up imaging. In both subgroups of patients undergoing either CF-RT or HF-RT, there was a statistically significant increase ($p < 0.05$) in breast volumes between baseline and 3 months follow-up. There were no statistically significant skin or volumetric changes of the untreated healthy breasts.

Conclusions: This is the first study utilizing 3D structured-light technology as a non-invasive and objective approach for the documentation of patients receiving breast radiotherapy. 3DSI offers potential as a non-invasive tool to objectively and precisely monitor the female breast in a radiooncological setting, allowing clinicians to objectively distinguish outcomes of different therapy modalities.

Keywords: Breast cancer, Breast-conserving therapy, Radiation therapy, Three-dimensional surface imaging, Breast imaging, Clinical studies, Volume measurements, Skin, Toxicity, Outcome

* Correspondence: konstantin.koban@med.uni-muenchen.de
[1]Division of Hand, Plastic and Aesthetic Surgery, University Hospital, LMU Munich, Pettenkoferstraße 8a, 80336 Munich, Germany
Full list of author information is available at the end of the article

Introduction

Adjuvant radiation therapy (RT) offers a significant benefit in preventing local recurrences and improves cancer-specific survival in patients undergoing breast-conserving therapy for early-stage breast cancer [1, 2]. Over the past decade the evaluation of hypofractionated treatment protocols has been of major interest in modern breast radiotherapy [3]. Several randomized trials (START A, START B trials and the Canadian trial) [4, 5] proved the safety and efficacy of hypofractionation (HF-RT), which recently has been introduced as the new standard of care in clinical practice [4–7]. Historically, the standard regimen consisted of conventional fractionated RT (CF-RT) using 25 fractions up to a dose of 50.0 Gy. Regarding primary endpoints like locoregional tumor relapse rates, there were no significant differences between the fractionation regimens in the randomized trials. However, regarding adverse effects, the HF-RT showed significantly less toxicities (breast induration/shrinkage, telangiectasia, and breast oedema) as compared to CF-RT. [8, 9] Most studies used clinical assessments, standardized questionnaires or standardized photographs to assess cosmetic outcome and adverse effects of breast RT. [10, 11] Nevertheless, it remains difficult to objectively assess side effects, like erythema, edema or fibrosis, which can negatively influence the shape, symmetry and appearance of the breast, and subsequently the patient's quality of life.

Tools that can objectively assess and document adverse events in order to identify the impact of different treatment regimens are therefore becoming increasingly important for future clinical studies. Recent technological developments have enabled the use of three-dimensional surface imaging (3DSI) as a viable solution to assess changes in breast contour and appearance [12–14]. 3DSI are powerful imaging devices that have already found widespread application in the field of plastic surgery, where they are advantageously affecting the process of planning and documenting breast-surgical procedures. One of the used imaging methods is depth sensor-based tracking of the body contour, which is also used for Surface Image Guided Radiation Therapy [15–18]. Other technologies, such as stereo-photogrammetric or structured light 3DSI, are also viable options for clinical applications [19]. The mobile Artec Eva 3D surface scanner (Artec 3D Inc., Luxembourg) is an affordable device that combines the latter two technologies. Its ability to create both, spatially highly accurate and textured 3D models with little effort, has already been successfully used in other clinical studies [20–23]. 3DSI allows to reproducibly assess changes in breast volume and appearance due to edema, fibrosis or erythema.

The aim of the present study was the application of an established 3DSI-based method routinely used in plastic surgery to document and quantify changes of the breast in patients receiving CF-RT and HF-RT, and to objectively confirm early onset of adverse effects during radiotherapy and early clinical follow-up.

Patients, materials and methods

Patient inclusion

Patients were invited to participate in this study on the day of their first visit at the department of Radiation Oncology, University Hospital, LMU Munich, Germany. Written informed consent was obtained from all patients. Patients receiving simultaneous bilateral breast radiotherapy were excluded from participation.

Radiation treatment

The breast clinical target volume (CTV) was delineated encompassing the glandular tissue of the breast, while the planning target volume (PTV) was defined by adding a margin of 5 mm in the transverse plane and 8 mm in cranial–caudal direction to the CT, according to the European Society for Radiotherapy and Oncology (ESTRO)-guidelines [24]. 3-dimensional conformal radiation therapy (3D-CRT) treatment planning was performed using the Oncentra Masterplan treatment planning system version 4.5.2 (Elekta AB, Sweden). All plans consisted of two opposing tangential beams for the breast with the addition of some subfields to increase dose homogeneity or to add the dose for the simultaneous integrated boost (SIB). The conventional fractionated RT (CF-RT) consisted of a total dose of 50 Gy in 25 fractions, while the hypofractionated regimens (HF-RT) was applied up to a dose of 40.05 Gy in 15 fractions. The boost to the tumor bed consisted of 10–16 Gy in 2 Gy single dose or a simultaneously integrated boost with a single dose of 0.5Gy/daily.

Imaging devices

The portable Artec Eva capture device (Artec 3D Inc., Luxembourg) was used for non-invasive 3DSI. It is depicted in Fig. 1. The surface scanner is equipped with structured light technology, which allows for a 3D point accuracy of up to 0.1 mm and a 3D resolution of up to 0.5 mm as specified by the manufacturer. With an operating distance ranging between 0.4 and 1 m, it enables the operator to rapidly capture localized areas of the human body [21–23, 25–27]. For the duration of the imaging process, the surface scanner was tethered via USB-interface to a commercially available capture Dell XPS 159560 laptop. The compact device was equipped with the Artec Studio Professional 12 software (Artec 3D Inc., Luxembourg) for surface capture and enabled subsequent image processing and analysis.

Fig. 1 The mobile structured-light surface scanner Artec Eva (Artec 3D Inc., Luxembourg) used for all imaging procedures

3D imaging and processing

One of three skilled operators (KCK, LE or ZL) informed the patients about the imaging procedure before conducting the baseline imaging session prior to the first radiation treatment. Subsequent images were acquired in weekly intervals for the duration of the treatment, as well as during the routine clinical follow-up where applicable.

Following a standardized protocol for patient positioning, imaging of the breast was conducted in an upright standing position. The patient's hands were placed on the hips, while the arms were left relaxed and the face was directed straight ahead. To prevent surface artefacts, the patients were requested to remove necklaces and clothing covering the torso prior to surface imaging. The operator instructed the patients to remain in the designated position and to keep as still as possible while breathing freely. Holding the surface scanner in one hand and the laptop placed on a side table directly adjacent to the patient, the operator proceeded to systematically capture all visible areas of the breast and front-facing torso. Imaging duration averaged to about 30 s. The raw data file was saved upon scan conclusion, followed by later registration and correct alignment of individual frames of the chest image resulting in a reconstruction of a textured 3D data file. An example of the final surface images can be seen in Figs. 2 and 3.

Assessment of breast changes

Usually, early toxicity and breast changes already occur during fractionated RT or within the first 12 weeks following RT. Skin erythema is the first sign of radiation dermatitis and its intensity varies with the radiation dose. While transient erythema may be seen even after a single fraction of radiation (2 Gy), hyperpigmentation, epitheliolysis, and desquamation only occur with increasing RT dose [28].

Late changes are considered to occur after 12 weeks following RT. There may be a variable latency period following acute/early changes during which the skin may appear normal and late effects like xeroderma, atrophy, telangiectasia, subcutaneous fibrosis which may develop after years. Fibrosis may develop, with progressive induration, edema, and thickening of the dermis and subcutaneous tissues [29]. The total radiation dose is critical in determining the severity of acute skin reactions, while the late effects are more influenced by the dose per fraction. Possible changes of the breast appearance as stated above were observed and recorded by the analysis of the textured 3D images after the conclusion of data acquisition.

3D volumetric analysis

The digital surface images of each patient were exported in the OBJ file format and superimposed by use of the closest iterative point algorithm within the Mirror Medical Imaging software (Canfield Sci., NJ, USA). Digital landmarks were placed by a trained examiner (KCK) for further analysis of breast changes. Breast dimensions were acquired by an automated software log reporting on the distances over surface between landmarks. Individual breast volume was quantified using another integrated software algorithm that digitally interpolated the chest wall to calculate the respective volume.

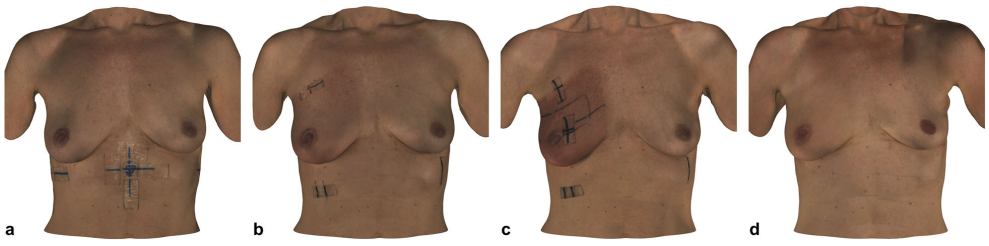

Fig. 2 Three-dimensional surface imaging overview of the front-facing torso of a patient receiving 50 Gy conventional fractionated radiotherapy with a subsequent 16 Gy boost of the right breast, as can be seen during baseline (a), week 3 (b), week 5 (c) and 3 months follow-up (d) imaging

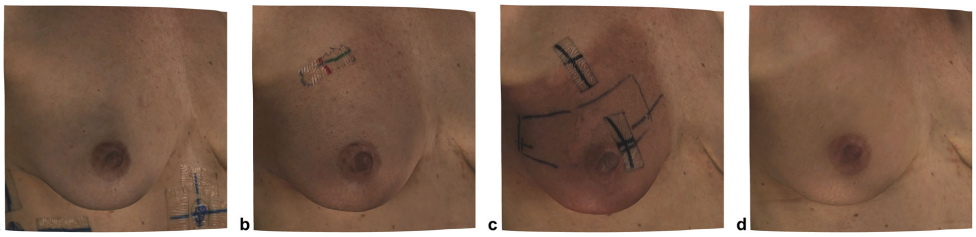

Fig. 3 Close-up image of the irradiated breast of the patient shown in Fig. 2, depicting in detail the breast appearance during baseline (a), week 3 (b), week 5 (maximum intensity of erythema) (c) and 3 months follow-up (d) imaging

Statistical analysis

We examined the breast appearance as well as volumetric breast measurements of all irradiated breasts. Changes during RT treatment and follow-up were analysed for all patients, as well as for different subgroups. The baseline was statistically compared with the subsequent imaging sessions and the clinical follow-up imaging. The untreated contralateral breasts were volumetrically analysed as control measurements to confirm scanner reproducibility. Subgroup analysis was performed regarding fractionation regimen (CF-RT vs HF-RT).

The frequency of changes in breast appearance was assessed using Fisher's exact test methodology. Changes regarding breast volume were examined using one-way repeated measures ANOVA for data where the assumptions of normal distribution and equal variance were met, else the Friedman repeated measures ANOVA on ranks was used. A p-value < 0.05 was considered statistically significant. All statistical analyses were conducted using the SigmaPlot Version 12.0 software package for scientific graphing and data analysis (Systat Software Inc., San José, CA, USA).

Results

Patient and tumor characteristics

For this study we enrolled thirty-eight (38) female patients. All women underwent radiation treatment and were imaged using 3DSI between November 2017 and September 2018. Patient and treatment characteristics are summarized in Table 1. Median age at diagnosis was 57 years (range: 30–80) and the median body mass index (BMI) was 23.3 (range: 17.2–28.5). The tumor side was right-sided in 16 cases (42.1%) and left-sided in 22 patients (57.9%). Overall, tumor stage was pTis in 4/38 women (10.6%), pT1 in 22/38 patients (57.9%), pT2 in 4/38 cases (10.6%) and pT3 in 1/38 patients (2.6%). Nodal status was negative in the majority of patients (78.9%, 30/38), positive in 5 patients (13.2%) and not evaluated in 3 patients (7.9%) with the diagnosis of DCIS (n = 2) or in the setting of recurrent disease (n = 1). Eleven patients underwent neoadjuvant systemic therapy due to triple negative breast cancer (n = 4), Her2-neu positive disease (n = 6) or a locally advanced cT4b tumor (n = 1).

Regarding the fractionation schemes, 15/38 patients (38.5%) received a normofractionated RT regimen (50Gy/25fractions) and 23/38 patients (60.5%) a hypofractionated

Table 1 Cohort characteristics

		38 patients	
		n	(%)
Age at diagnosis (years)	< 50	9	(23.7)
	51–60	13	(34.2)
	61–70	6	(15.8)
	> 71	10	(26.3)
	median age (years)	57.0	
Tumor side	Left	22	(57.9)
	Right	16	(42.1)
Surgery	BCS	36	(94.7)
	Mastectomy with immediate reconstruction	2	(5.3)
Tumour size	ypT0	7	(18.4)
	pTis	4	(10.6)
	pT1	22	(57.9)
	pT2	4	(10.6)
	pT3	1	(2.6)
Nodal status	pN0	30	(78.9)
	pN+	5	(13.2)
	pNx	3	(7.9)
Grade	G1	5	(13.2)
	G2–3	33	(86.8)
Hormone Receptor	positive	27	(71.1)
	negative	10	(26.3)
	unknown (DCIS)	1	(2.6)
Her2/neu Status	positive	9	(23.7)
	negative	27	(71.0)
	unknown (DCIS)	2	(5.3)
Radiotherapy regimen	Normofractionated (50Gy/25fx)	15	(39.5)
	Hypofractionated (40Gy/15fx)	23	(60.5)
Boost	no	21	(55.3)
	yes	17	(44.7)
BMI	median (range)	22.3	(17.2–28.5)

Table 2 Assessment of breast changes (skin erythema) during the treatment course and clinical follow-up at 3 months

Timepoint	baseline	week 1	week 2	week 3	week 4	week 5	week 6	week 7	follow-up
Overall	0.0	2.9	14.7	36.8	77.3	100.0	100.0	66.7	3.7
CF-RT	0.0	0.0	7.7	46.7	92.9	100.0	100.0	66.7	0.0
HF-RT	0.0	4.8	19.0	30.4	50.0	NA	NA	NA	5.6

All results are expressed in percent of patients ($n = 38$)

RT (40Gy/15fx). Moreover, 17 patients (44.7%) received a consecutive boost irradiation to the tumor bed or a simultaneously integrated boost (n = 2).

Assessment of breast changes

A total of 214 imaging sessions were conducted. None of the patients receiving CF-RT or HF-RT showed signs of a skin reaction during the baseline imaging session. Details on the incidence of changes in breast appearance are displayed in Table 2.

When examining the overall changes regarding breast appearance, we found localised skin erythema in 22 out of 38 cases (57.9%). One patient (2.6%) of the entire cohort suffered from epitheliolysis of the nipple-areolar complex, which subsided completely before the final follow-up imaging session at 3 months after RT. Moreover, all skin reactions were observed during a maximum of 4 consecutive imaging sessions. Changes in breast appearance were mostly self-limited after the end of the radiation treatment with only one observed case (3.7%) of persistent erythema during clinical follow-up.

Regarding the influence of the different fractionation schemes, 1 out of 15 patients receiving CF-RT (6.7%) showed no signs of skin reaction, while 14 out of 15 women (93.3%) experienced skin erythema within the target volume (see Figs. 2 and 3). The median starting point was during the third week of radiation, with a maximum peak during the fifth week. The erythema decreased until the sixth week of radiation treatment and had a median duration of 2 weeks. In contrast, 15 out of 23 patients undergoing HF-RT (65.2%) showed no signs of any skin reaction, while eight out of 23 patients (34.8%) exhibited localised skin erythema. The median starting point was earlier than in CF-RT and began in the second week of radiation, with a maximum peak in the third week and the end point during the fourth week of radiation treatment. The duration of the skin reaction was similar to CF-RT, with a median duration of 2 weeks.

We observed changes in breast appearance during week 3 of RT in 46.7% of patients receiving CF-RT, and in 30.4% of patients receiving HF-RT. When examined using Fisher's exact test methodology, this difference was not statistically significant ($p = 0.165$). None of the patients undergoing CF-RT presented with changes in breast appearance during the clinical follow-up visit, whereas one single HF-RT patient (5.6%) exhibited persistent localised redness. This difference was also not statistically significant ($p = 0.805$). However, patients receiving CF-RT showed a statistically significant higher frequency of changes in breast appearances when compared to HF-RT (93.3% versus 34.8%, $p = 0.003$) if all observed imaging sessions were considered.

3D volumetric analysis

The detailed volumetric results are listed in Table 3. The mean breast volume for the entire cohort during baseline imaging was 379 ± 196 mL, as compared to 391 ± 198 mL during week 3 of RT and 437 ± 224 mL during clinical follow-up at 3 months. When using the Friedman test to compare the volumetric results of the treated breast for the entire cohort, we found a statistically significant change in breast volume between the examined imaging sessions ($p < 0.001$). Subsequent use of Dunn's method of multiple comparisons showed a statistically significant increase ($p < 0.05$) of breast volumes between both, baseline and follow-up at 3 months, as well as between week 3 and follow-up imaging. There were no statistically significant changes in breast volume when examining the untreated healthy breasts ($p = 0.708$).

Regarding the influence of the different fractionation schemes, in patients undergoing CF-RT, the mean breast volume during baseline imaging was 387 ± 171 mL, as compared to 416 ± 183 mL during week 3 and 443 ± 212 mL during clinical follow-up at 3 months ($p < 0.001$). Subsequent analyses showed a statistically significant

Table 3 Assessment of volumetric breast changes during the treatment course and clinical follow-up at 3 months for the entire cohort and the two subgroups, receiving either conventionally fractionated RT (CF-RT) or hypofractionated RT (HF-RT)

	baseline	week 3	follow-up
Entire cohort (treated breast)	379 ± 196	391 ± 198	437 ± 224
Entire cohort (untreated breast)	382 ± 203	382 ± 205	382 ± 208
CF-RT (treated breast)	387 ± 171	416 ± 183	443 ± 212
CF-RT (untreated breast)	363 ± 174	370 ± 184	338 ± 160
HF-RT (treated breast)	375 ± 211	379 ± 209	434 ± 236
HF-RT (untreated breast)	392 ± 220	389 ± 220	404 ± 229

All results are given as mean ± sd (standard deviation) in millilitres (mL)

increase ($p < 0.05$) of breast volumes between baseline and follow-up imaging. Similarly, patients undergoing HF-RT, had a mean breast volume during baseline imaging of 375 ± 211 mL, 379 ± 209 mL during week 3, and 434 ± 236 mL during clinical follow-up at 3 months, which was a statistically significant increase ($p < 0.05$) between baseline and follow-up imaging.

Discussion

In the present study, weekly 3DSI of patients undergoing either CF-TR or HF-RT was conducted for the duration of RT treatment and on clinical follow-up. The portable Artec Eva scanner provided reproducible 3D surface images for analysis of breast volume and changes in breast appearance. A total of 38 patients were enrolled and 214 breast imaging sessions were performed.

While a greater percentage of patients receiving CF-RT showed changes in breast appearance during week 3 of RT when compared to patients receiving HF-RT (46.7% versus 30.4%), this difference was not statistically significant ($p = 0.165$). No patients having received CF-RT presented with changes in breast appearance during the clinical follow-up visit, whereas a single patient having received HF-RT, exhibited localised redness (0.0% versus 5.6%, $p = 0.805$). However, patients receiving CF-RT showed a statistically significant higher frequency of changes in breast appearances when compared with HF-RT (93.3% versus 34.8%, $p = 0.003$) throughout all observed imaging sessions.

When assessing the volumetric breast changes during the treatment course and clinical follow-up at 3 months for the entire cohort, we found a statistically significant ($p < 0.05$) volumetric increase between both baseline and follow-up imaging, as well as between week 3 and follow-up imaging. In both subgroups of patients undergoing either CF-RT or HF-RT, there was a statistically significant increase ($p < 0.05$) in breast volumes between baseline and 3 months follow-up imaging. As a proof of principle, we found no statistically significant changes in breast volumes when examining the untreated healthy breast.

To the best of our knowledge, this is the first study utilizing 3D structured-light technology as a non-invasive and objective approach for the documentation of side effects during breast radiotherapy. Quantitative metrics derived from 3D surface images allowed to compare the differences regarding cosmetic outcome and early effects of radiation toxicity of different fractionation regimens. While the use of 3DSI enables the assessment of the occurrence and development of skin changes, such as hyperpigmentation and erythema, the software lacks an automated algorithm to analyse the chromatic properties of these changes. Although such tools have been described in other works [30, 31], the application of such tools in conjunction with standardized 3DSI might further improve objective assessments in future. Applying this technology in clinical studies in the field of radiation oncology could offer an additional, standardized method to objectively assess and document side effects, such as variations in breast volume or skin deterioration, and match those to subjective evaluated parameters of patient reported outcome measurements (PROMS).

In comparison to conventional photography, studies have shown the superiority of objective and reproducible measurements of 3DSI [32, 33]. The 3D imaging device used in the present setting is a portable system that works with structured light imaging and photogrammetric technology, thus enabling fast capturing of a complete 3D surface model of the front-facing thorax within 30 s. During the scanning process itself, the distance from the patient to the camera is shown on the computer screen for better reproducibility. In addition, the practicability is very good, as data processing takes only 2–5 min until final evaluation. This could be even faster, if a more powerful computer was used in clinical practice. However, a drawback of the Artec software is the lack of an accompanying user-friendly medical patient database and comprehensive assessment and evaluation tools for detailed analysis. By importing the scans into the Mirror medical imaging software, we were able to use its database function and analysis tools for greater ease of use.

The texture quality is excellent even under normal light conditions and allows a detailed assessment of skin structure. The system has an integrated light source, which provides a high frequency sequential flashing light, which eliminates the need for extra light adjustments in the background. However, the sequential flashing lights could be unpleasant during patient consultation and its use is not recommended in patients suffering from epilepsy. Regarding susceptibility to involuntary movements, sensitivity was significantly reduced when patients were asked to remain in a relaxed body pose.

The volumetric measurement capabilities of the Artec Eva scanner were previously examined in a cadaveric model, where predefined amounts of injected volume were analysed in various facial regions [20, 21]. The imaging device was found to provide highly accurate results, even when dealing with as little as milliltres of injected volume. Thus, it can be assumed that the scanner used in this study provides very reliable results regarding volumetric changes of both the irradiated as well as the untreated breast.

Nevertheless, the system has also some remaining limitations. Although 3DSI offers a low-priced and radiation-free method of assessing body contour and volumetric developments when compared to MRI or CT, the technology only

allows body surfaces to be registered. For this reason, it is necessary to compare at least two images to document the relative difference between surfaces. Depending on the technology and software used for imaging, measurements regarding absolute breast volumes have been known to show a higher variance when compared to MRI and CT, and therefore remain inconclusive [34]. Another limitation is the process of manual landmark placement to digitally mark breast boundaries in patients with a high BMI or severe breast ptosis, especially when regarding the inframammary fold and lateral breast border. In the present study, the breast volume was measured by digitally calculating the space enclosed by the 3D surface image of the breast and a digital surface representing the chest wall. The spatial accuracy of this interpolated surface relies heavily on correctly identified breast borders. However, a trained examiner performed the placement of landmark points using a standardized operating procedure, and as a method for internal validation and proof of principle, the volume of untreated contralateral breasts was measured to confirm reproducibility. Over the entire study duration, there were no significant volume changes in the respective healthy contralateral breasts. Physiological volumetric changes of the healthy breast could occur due to changes in body weight or through the influence of the menstrual cycle [35], although they were observed to be negligibly small. Thus, the surface scanner can be assumed to precisely gauge the captured breast volume.

Conclusion

This is the first study utilizing 3D structured-light technology as a non-invasive and objective approach for the documentation of patients receiving breast radiotherapy. Quantitative metrics derived from 3D surface images allowed to compare the differences regarding cosmetic outcome and early effects of conventionally fractionated (CF-RT) and hypofractionated radiation treatment (HF-RT). 3DSI offers potential as a non-invasive tool to objectively monitor the female breast in a radiooncological setting, allowing clinicians to objectively and precisely distinguish outcomes of different therapy modalities.

Acknowledgements
We would like to thank Anna Ruprecht for her assistance regarding patient management and participant enrolment. We would also like to thank Anna Ruprecht and Ya Xu for their assistance with the 3D imaging procedures.

Authors' contributions
KCK, LE and ZL conducted all surface imaging procedures and subsequent image processing. KCK conducted all digital analyses and performed the statistical analysis. SC and TLS made substantial contributions to the conception and design of the work. REG, LE, KCK, and SC were major contributors in drafting and writing the manuscript. MP, SS, CB, SC were responsible for radiation treatment, acquired written informed consent from all patients, and clinically evaluated the observed skin changes during radiation treatment. The author(s) read and approved the final manuscript.

Funding
The authors received no financial support for the research, authorship, and/or publication of this article. None of the other authors listed have any commercial associations or financial disclosures that might pose or create a conflict of interest with the methods applied or the results presented in this article.

Availability of data and materials
The datasets generated and/or analysed during the current study are not publicly available due to the General Data Protection Regulation (GDPR) but are available from the corresponding author on reasonable request.

Ethics approval and consent to participate
This study was conducted in accordance with the Declaration of Helsinki and with approval from the Ethics Committee of the Ludwig-Maximilians-University Munich (Reference Number 17–630). Written informed consent was obtained from all patients prior to study enrolment.

Consent for publication
Written informed consent for image publication was obtained from the patient depicted in the figures.

Competing interests
The authors declare that they have no competing interests.

Author details
[1]Division of Hand, Plastic and Aesthetic Surgery, University Hospital, LMU Munich, Pettenkoferstraße 8a, 80336 Munich, Germany. [2]Department of Radiation Oncology, University Hospital, LMU Munich, Munich, Germany.

Received: 20 December 2019 Accepted: 18 February 2020
Published online: 28 February 2020

References

1. Corradini S, et al. Adjuvant radiotherapy after breast conserving surgery – a comparative effectiveness research study. Radiother Oncol. 2015;114:28–34.
2. Corradini S, et al. Mastectomy or breast-conserving therapy for early breast Cancer in real-life clinical practice: outcome comparison of 7565 cases. Cancers (Basel). 2019;11(160).
3. Chitapanarux I, et al. Conventional versus hypofractionated postmastectomy radiotherapy: a report on long-term outcomes and late toxicity. Radiat Oncol. 2019;14:175.
4. Whelan TJ, et al. Long-term results of Hypofractionated radiation therapy for breast Cancer. N Engl J Med. 2010;362:513–20.
5. Haviland JS, et al. The UK standardisation of breast radiotherapy (START) trials of radiotherapy hypofractionation for treatment of early breast cancer: 10-year follow-up results of two randomised controlled trials. Lancet Oncol. 2013;14:1086–94.
6. Brunt AM, et al. Acute skin toxicity associated with a 1-week schedule of whole breast radiotherapy compared with a standard 3-week regimen delivered in the UK FAST-forward trial. Radiother Oncol. 2016;120:114–8.
7. Yarnold JR. First results of the randomised UK FAST trial of radiotherapy hypofractionation for treatment of early breast cancer (CRUKE/04/015). Radiother Oncol. 2011;100:93–100.
8. Hopwood P, et al. Comparison of patient-reported breast, arm, and shoulder symptoms and body image after radiotherapy for early breast cancer: 5-year follow-up in the randomised standardisation of breast radiotherapy (START) trials. Lancet Oncol. 2010;11:231–40.
9. Shaitelman SF, et al. Three-year outcomes with Hypofractionated versus conventionally fractionated whole-breast irradiation: results of a randomized, Noninferiority Clinical Trial. J Clin Oncol. 2018;36:3495–503.
10. Agrawal RK, et al. The UK standardisation of breast radiotherapy (START) trial B of radiotherapy hypofractionation for treatment of early breast cancer: a randomised trial. Lancet. 2008;371:1098–107.
11. Matuschek C, et al. Long-term cosmetic outcome after preoperative radio –/chemotherapy in locally advanced breast cancer patients. Strahlentherapie und Onkol. 2019;195:615–28.
12. Tsay C, Zhu V, Sturrock T, Shah A, Kwei S. A 3D Mammometric comparison of implant-based breast reconstruction with and without Acellular dermal matrix (ADM). Aesthet Plast Surg. 2018;42:49–58.

13. Tepper OM, et al. 3D analysis of breast augmentation defines operative changes and their relationship to implant dimensions. Ann Plast Surg. 2009; 62:570–5.
14. Koban KC, Frank K, Etzel L, Schenck TL, Giunta RE. 3D Mammometric changes in the treatment of idiopathic Gynecomastia. Aesthet Plast Surg. 2019;43:616–24.
15. Reitz D, et al. Real-time intra-fraction motion management in breast cancer radiotherapy: analysis of 2028 treatment sessions. Radiat Oncol. 2018;13:128.
16. Carl G, et al. Optical surface scanning for patient positioning in radiation therapy: a prospective analysis of 1902 fractions. Technol Cancer Res Treat. 2018;17:153303381880600.
17. Schonecker S, et al. Treatment planning and evaluation of gated radiotherapy in left-sided breast cancer patients using the CatalystTM/ SentinelTM system for deep inspiration breath-hold (DIBH). Radiat Oncol. 2016;11:143.
18. Hamming VC, et al. Evaluation of a 3D surface imaging system for deep inspiration breath-hold patient positioning and intra-fraction monitoring. Radiat Oncol. 2019;14:125.
19. Tzou CHJ, et al. Comparison of three-dimensional surface-imaging systems. J Plast Reconstr Aesthetic Surg. 2014;67:489–97.
20. Cotofana S, et al. The surface-volume coefficient of the superficial and deep facial fat compartments. Plast Reconstr Surg. 2019;143:1605–13.
21. Koban KC, et al. Precision in 3-dimensional surface imaging of the face: a handheld scanner comparison performed in a cadaveric model. Aesthetic Surg J. 2019;39:NP36–44.
22. Seminati E, et al. Validity and reliability of a novel 3D scanner for assessment of the shape and volume of amputees' residual limb models. PLoS One. 2017;12:e0184498.
23. Modabber A, et al. Influence of connecting two standalone Mobile three-dimensional scanners on accuracy comparing with a standard device in facial scanning. J Oral Maxillofac Res. 2016;7:e4.
24. Offersen BV, et al. ESTRO consensus guideline on target volume delineation for elective radiation therapy of early stage breast cancer. Radiother Oncol. 2015;114:3–10.
25. Koban KC, et al. Validation of two handheld devices against a non-portable three-dimensional surface scanner and assessment of potential use for intraoperative facial imaging. J Plast Reconstr Aesthetic Surg. 2019. https://doi.org/10.1016/j.bjps.2019.07.008.
26. Schenck TL, et al. Updated anatomy of the buccal space and its implications for plastic, reconstructive and aesthetic procedures. J Plast Reconstr Aesthetic Surg. 2018;71:162–70.
27. Grant CA, Johnston M, Adam CJ, Little JP. Accuracy of 3D surface scanners for clinical torso and spinal deformity assessment. Med Eng Phys. 2019;63: 63–71.
28. Borm KJ, et al. Acute radiodermatitis in modern adjuvant 3D conformal radiotherapy for breast cancer - the impact of dose distribution and patient related factors. Radiat Oncol. 2018;13:218.
29. Liang X, et al. Prognostic factors of radiation dermatitis following passive-scattering proton therapy for breast cancer. Radiat Oncol. 2018;13:72.
30. Partl R, Lehner J, Winkler P, Kapp KS. Testing the feasibility of augmented digital skin imaging to objectively compare the efficacy of topical treatments for radiodermatitis. PLoS One. 2019;14:1–11.
31. Partl, R. et al 128 SHADES of RED: Objective remote assessment of radiation dermatitis by augmented digital skin imaging. Stud Health Technol Inform 236, 363–374 (IOS Press, 2017).
32. Lekakis G, Claes P, Hamilton G, Hellings P. Three-dimensional surface imaging and the continuous evolution of preoperative and postoperative assessment in Rhinoplasty. Facial Plast Surg. 2016;32:088–94.
33. Lane C, Harrell W. Completing the 3-dimensional picture. Am J Orthod Dentofac Orthop. 2008;133:612–20.
34. Choppin SB, Wheat JS, Gee M, Goyal A. The accuracy of breast volume measurement methods: a systematic review. Breast. 2016;28:121–9.
35. Wang C, et al. Menstrual cycle-related fluctuations in breast volume measured using three-dimensional imaging: implications for volumetric evaluation in breast augmentation. Aesthet Plast Surg. 2019;43:1–6.

Publisher's Note

5.2 Publikation 2

Etzel, L., Schenck, T.L., Giunta, R.E., Li, Z., Xu, Y., Koban, K.C.: Digital Leg Volume Quantification: Precision Assessment of a Novel Workflow Based on Single Capture Three-dimensional Whole-Body Surface Imaging. Journal of Digital Imaging. 34, 1171–1182 (2021). https://doi.org/10.1007/s10278-021-00493-8

Journal of Digital Imaging (2021) 34:1171–1182
https://doi.org/10.1007/s10278-021-00493-8

ORIGINAL PAPER

Digital Leg Volume Quantification: Precision Assessment of a Novel Workflow Based on Single Capture Three-dimensional Whole-Body Surface Imaging

Lucas Etzel[1] · Thilo L. Schenck[1] · Riccardo E. Giunta[1] · Zhouxiao Li[1] · Ya Xu[1] · Konstantin C. Koban[1]

Received: 7 September 2020 / Revised: 3 June 2021 / Accepted: 5 July 2021 / Published online: 28 September 2021

Abstract
Whole-body three-dimensional surface imaging (3DSI) offers the ability to monitor morphologic changes in multiple areas without the need to individually scan every anatomical region of interest. One area of application is the digital quantification of leg volume. Certain types of morphology do not permit complete circumferential scan of the leg surface. A workflow capable of precisely estimating the missing data is therefore required. We thus aimed to describe and apply a novel workflow to collect bilateral leg volume measurements from whole-body 3D surface scans regardless of leg morphology and to assess workflow precision. For each study participant, whole-body 3DSI was conducted twice successively in a single session with subject repositioning between scans. Paired samples of bilateral leg volume were calculated from the 3D surface data, with workflow variations for complete and limited leg surface visibility. Workflow precision was assessed by calculating the relative percent differences between repeated leg volumes. A total of 82 subjects were included in this study. The mean relative differences between paired left and right leg volumes were $0.73 \pm 0.62\%$ and $0.82 \pm 0.65\%$. The workflow variations for completely and partially visible leg surfaces yielded similarly low values. The workflow examined in this study provides a precise method to digitally monitor leg volume regardless of leg morphology. It could aid in objectively comparing medical treatment options of the leg in a clinical setting. Whole-body scans acquired using the described 3DSI routine may allow simultaneous assessment of other changes in body morphology after further validation.

Keywords 3D surface scanner · Leg volumetry · Device validation · Whole-body scan · Leg edema · Structured-light scanning

Introduction

Three-dimensional surface imaging (3DSI) is increasingly gaining recognition as a valuable tool for the objective documentation of volumetric changes in body morphology. The use of 3D scanning has recently been investigated regarding its usefulness for the documentation of body shape in bariatric surgery [1]. It is also being used for ever more complex tasks in maxillofacial surgery [2] and is finding application for augmented reality and virtual reality [3]. Clinicians of a growing number of medical disciplines effectively apply this radiation-free and cost-efficient technology to monitor specific anatomical regions, such as the breast [4, 5], face [6, 7], or leg [7, 8].

However, only those parts of the body that are visible during the scanning process can be mapped reliably. This is especially relevant when wanting to assess the lower extremity, as part of the surface of each leg may be obscured by the other leg [9].

A variety of investigations have been conducted to identify an objective, fast, cost-efficient, precise, and non-invasive method to measure leg volume. Presently used methods to quantify limb volume changes include standardized tape measurements to estimate volume, water displacement, perometry, computer tomography (CT), and magnetic resonance imaging (MRI). Numerous studies have compared these methods [8, 10–15]. While they are all routinely applied in clinical practice, each comes with certain benefits and limitations. Tape measurements have been shown to be of

✉ Lucas Etzel
lucas.etzel@med.uni-muenchen.de

[1] Division of Hand, Plastic and Aesthetic Surgery, University Hospital, LMU Munich, Pettenkoferstraße 8a, 80336 Munich, Germany

limited reliability [11]. Volume measurements through use of water displacement represent a cumbersome method that is unsuited for patients with open skin lesions of the leg [12, 13]. The use of MRI or CT offers the beneficial ability to monitor the sub-surface morphology. However, these methods will remain time-consuming or invasive and are thus less useful for routine monitoring of leg volume.

To find an objective and simple alternative to these methods, recent studies have examined the use of 3DSI for leg volume analyses [8, 9, 13, 16, 17]. Clinical application for the documentation of body morphology is associated with various benefits. The technology provides a contact- and radiation-free method to create digital surface maps. As such it is fast, cheap, and non-invasive when compared to CT and MRI. 3D scanning can be outsourced to trained personnel other than the treating physician. It requires less effort than traditional measurement techniques such as water displacement or when collecting large data samples using a tape measure or calipers.

By following a standardized whole-body acquisition process, the use of 3DSI supplies a digital copy of the visible surface. This can be analyzed to monitor the shape and size of the entire human body regarding distances, surface areas, and total body or segmental volumes [18–21]. This application of handheld 3D scanners can allow the assessor to monitor multiple areas of interest without the need to individually scan every anatomical region in question [19, 22]. It also offers the benefit of simultaneously documenting other anatomical areas which may prove to be of interest during a later clinical evaluation.

While various studies have examined the use of 3DSI to digitally assess leg morphology, it is common practice to either reposition each leg for individual scanning [8, 9, 17], or to scan one pose with a defined inter-foot distance [23]. Depending on leg morphology, such a technique may however still fail to allow visibility of the entire leg circumference in subjects with high leg volume. This creates the need for a standardized pose that allows as much leg visibility as possible without repositioning and re-scanning multiple areas. The concept of gathering leg volume measurements from whole-body 3DSI has been addressed in several studies [24, 25]. However, there are types of body morphology that do not allow for full leg visibility with this technique. In such cases the use of an estimation process is necessary to fill holes in the 3D leg surface data.

Our solution included the development of a workflow to acquire a complete set of whole-body 3D surface data during a single scanning procedure, i.e., without merging individual 3D scans of parts of the body. These data were then used to precisely quantify bilateral leg volume regardless of leg shape and volume, while allowing further analysis of other anatomical regions of interest. To cope with varying leg morphology, two workflow variations were devised. For subjects in which the entire circumference of each leg was visible in the standard pose, we applied the complete leg visibility workflow variation. In cases where leg morphology caused insufficient exposure of the leg surface, a limited leg visibility workflow variation was applied to estimate the missing surface data and thus still enable precise leg volume quantification. With these workflow variations, we were able to compare leg volumes for subjects with a wide range of leg morphologies.

In this study, the authors wanted to investigate the usefulness of a 3DSI-based workflow for the objective documentation of leg volume. The aim of this study was to describe and apply a novel workflow and to assess workflow precision while comparing two workflow variations. The workflow variations were compared to assess whether the method can precisely gauge leg volume regardless of leg morphology. Our objectives were to collect two repeated samples of bilateral leg volumes from all subjects included in a suitable study cohort and to calculate the respective mean volumes as well as the absolute and relative percent differences between these paired samples of volumetric data.

Patients, Materials, and Methods

Study Population

Patients over the age of 18 years who presented themselves for medical consultation at our hospital department between July 2017 and January 2020 were approached for study enrollment. The subjects were recruited from a sample of patients receiving body-contouring surgery, patients with lipedema, as well as other plastic surgical patients without leg issues, e.g., breast cancer patients. We aimed to recruit a cohort with a wide body-mass-index (BMI) range, and to include subjects with diverse leg morphology and varying degrees of leg volume. Volunteers were excluded if presenting with orthopedic or neurological conditions likely to intefere with the imaging procedure.

Data Collection and Workflow Protocol

Two sets of whole-body 3D surface data were acquired for each subject. After a first 3D surface scan, subjects were allowed to move and were then repositioned in the same pose for the second scan. We were thus able to examine the reproducibility of measurements.

By adhering to the following standardized imaging procedure and two variations of a novel leg volume analysis workflow, paired bilateral leg volume measurements were recorded for each participant. Prior to 3DSI, the respective imaging operator briefed the subject on the imaging

procedure, obtained written informed consent, and recorded data regarding age, sex, and BMI.

The handheld and wireless structured-light Thor3D Scanner (Thor3D, Moscow, Russia) was used together with an automated turntable (Thor3D, Moscow, Russia) as a portable consumer grade whole-body imaging system. Technical details as specified by the manufacturer included a scanning accuracy of up to 0.2 mm and a resolution of up to 1 mm with a frame rate of up to 10 per second. The motorized turntable was capable of a rotational speed of 0.25–6.5 rpm. It was manually marked with areas for standardized foot positioning at an inter-foot distance of about 40 cm.

To ensure high scan quality, the subjects were requested to remove all jewelry and to tie back long hair as well as to remove all clothing apart from tight fitting undergarments. 3DSI was conducted with the subjects standing freely in an upright position with arms spread and the hands resting on the hips. The subjects were instructed to breathe freely for the duration of 3DSI, while trying to alter their body pose as little as possible. Subjects were requested to keep their eyes open, as preliminary tests showed that closed eyes increased the amount of swaying motion. At a scanning distance of about 1 m, the imaging operator performed a systematic scan sequence by moving the imaging focus from the feet toward the head. While taking advantage of the turntable rotation to circumferentially map all visible surface areas of the body, each set of whole-body 3D surface data was acquired in a single scanning procedure. The mean scan duration was about 45 s. The resulting raw data were transferred via USB flash drive to a commercial desktop computer running Microsoft Windows 10 for data processing.

Using predetermined settings based on those recommended by the manufacturer for whole-body scanning, data were processed using the Thor3D Windows desktop software and subsequently exported into the Geomagic 2014 software (3D Systems, Rock Hill, SC, USA). To allow for comparison, each resulting set of whole-body 3D surface data needed to be rotated to a standard orientation. To this purpose, the visible area of the flat turntable surface from each scan was aligned with a predefined transverse plane object at the coordinate system origin. The whole-body 3D surface data were then axially rotated to correctly face the frontal plane. The alignment process of the whole-body 3D surface data is depicted in Fig. 1.

Leg segments were obtained for volumetric analysis by cropping the 3D surface data above and below transverse planes at the height of the infragluteal fold and the lateral malleolus, respectively. The transverse planes were set at a specific height in millimeters over the point of origin as defined by the turntable surface. These heights were then used for each leg of both sets of whole-body 3D surface scans. Thus, we were able to reproducibly crop the leg segments for volumetric analysis within the 3D surface data of the same subject. In cases where the two resulting legs segments were completely separate, the 3D surface data were submitted to the complete leg visibility workflow. In cases where the cropped segments showed fusing of the legs in the medial thigh area, the 3D surface data were submitted to the limited leg visibility workflow. This included an extra step of data processing, in which the computed 3D surface data were separated in the median sagittal plane between the fused legs. To estimate the medial boundaries of each respective leg, the missing 3D surface data were then interpolated by applying the flat plane hole-filling algorithm within the Geomagic 2014 software. An example of a leg segment from whole-body 3D surface data processed using the limited leg visibility workflow variation is highlighted in Fig. 2. Subsequently, the mesh doctor function within the Geomagic 2014 software was applied for scan cleanup by means of spike-edge removal and small hole filling, before saving each separated leg into individual.stl files.

The final leg segments were exported into the Mirror medical imaging software (Canfield Scientific Inc, Parsippany, NJ, USA). The in-software volume measurement function was used to quantify the leg segments. The output in the Mirror analysis log was saved in a .csv file ready for data transformation.

Study Data Analysis

Data transformation and analysis, as well as scientific writing and table and graph creation, was conducted using the R software environment for statistical computing and graphics (version 4.0.0) [27] with RStudio (Version 1.3.1093) [28], R Markdown [29], and selected R packages [30–33]. A p value < 0.05 was considered statistically significant. Sample normality was analyzed using q-q plots and the Shapiro–Wilk test. All analyses were conducted separately for the left and right leg.

Prior to descriptive and statistical analysis, the collected leg volume data were combined with the demographic data of each subject. The demographic data were analyzed for the entire study cohort, and, for both, the complete and limited leg visibility workflow subgroups.

The mean value of paired leg volume measurements from each subject was assessed for the entire study cohort. By splitting the study cohort into five subgroups based on the WHO BMI classification [34], a boxplot was created to graphically analyze the calculated mean volumes in relation to subject BMI. The BMI subgroups were defined by the relevant value in kilogram per square meter (kg/m^2): normal weight (18.5–24.9), pre-obesity (25.0–29.9), obesity class I (30.0–34.9), obesity class II (35.0–39.9), and obesity class III (above 40).

The difference between the paired absolute leg volume measurements from each subject was analyzed for the entire

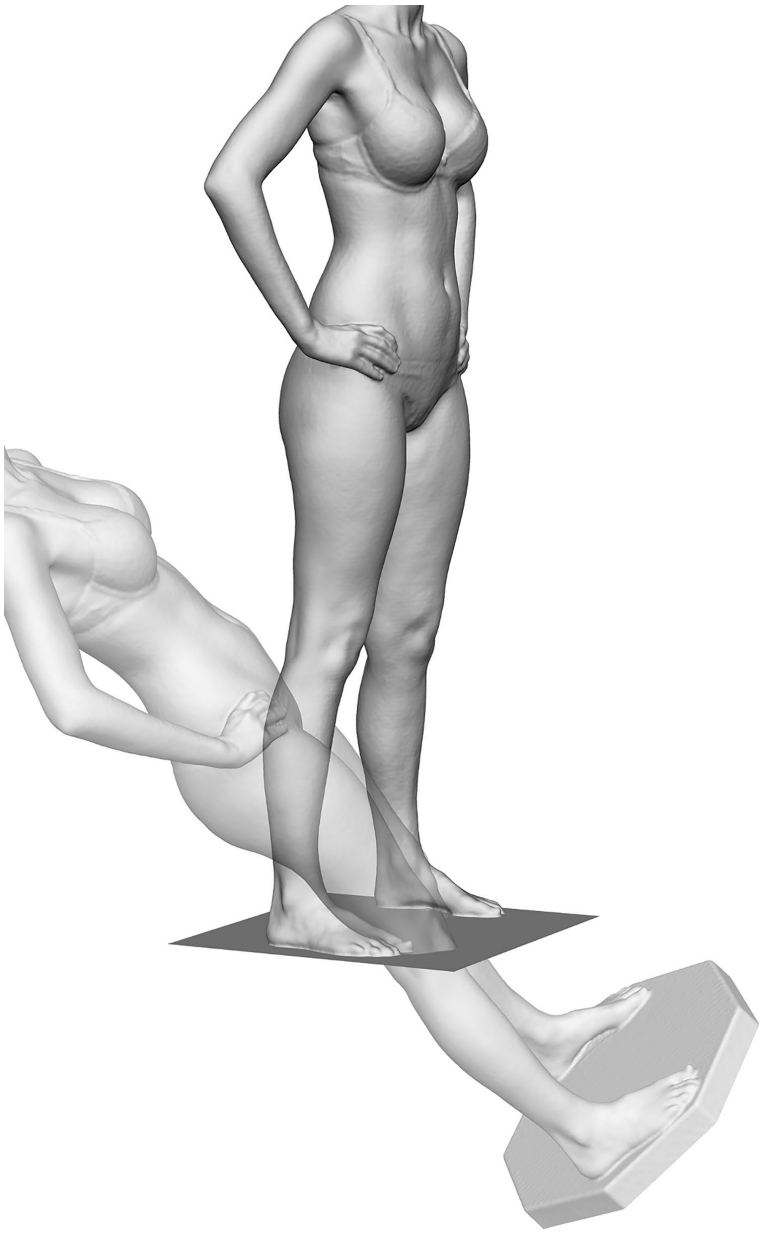

Fig. 1 Orientation of a whole-body scan by aligning the flat turntable surface with a predefined transverse plane object at the coordinate system origin

study cohort as well as for both the complete and limited leg visibility workflow subgroups. Using the paired *t*-test to compare the volume samples, we calculated the mean differences between the samples with 95% confidence intervals.

Furthermore, the relative differences between each pair of repeated measurements were calculated as a percentage of the absolute difference between paired leg volumes divided by the mean value of both measurements. By calculating

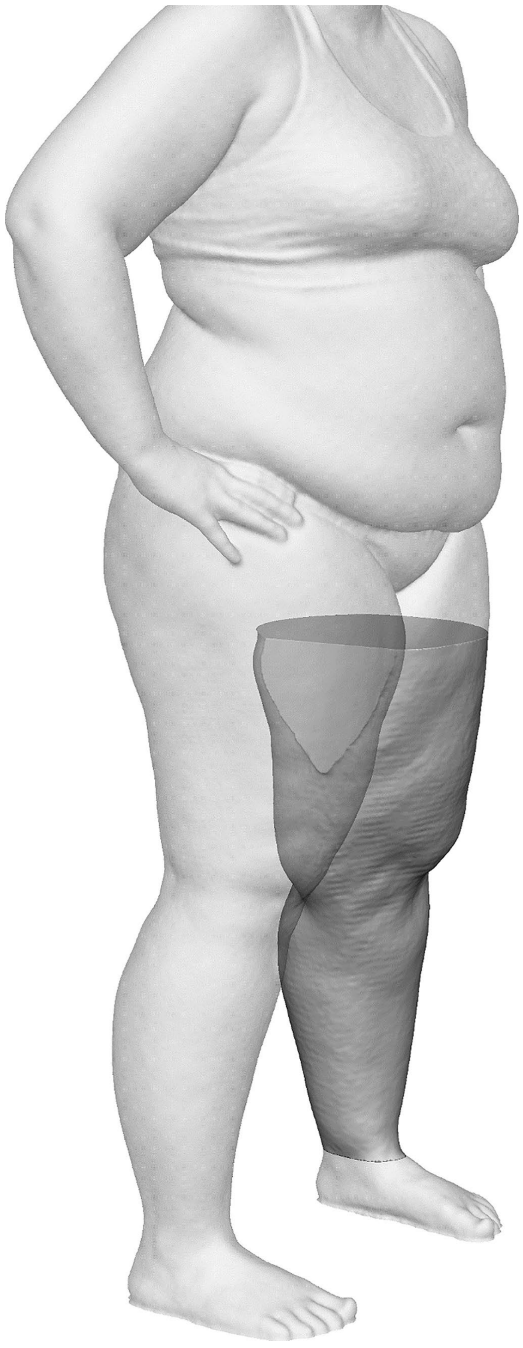

Fig. 2 Exemplary illustration of the left leg segment of a whole-body scan processed using the limited leg visibility workflow variation

these relative differences, we could compare the repeated measurements regardless of the varying absolute leg volumes of each subject. We deemed lower values of relative difference between repeated leg volume measurements to indicate an increasing level of precision.

A boxplot was created to graphically analyze the relative difference between each pair of repeated measurements depending on the respective use of workflow. The Wilcoxon test was used to test for statistical significance between the scores of both workflow samples for each leg.

Results

Workflow Application

By applying the described workflow, paired sets of whole-body 3D surface data were successfully processed and analyzed for each of the 82 study participants. As illustrated for a single subject in Fig. 3, the two sets of volumetric data for each leg were compared. The respective mean

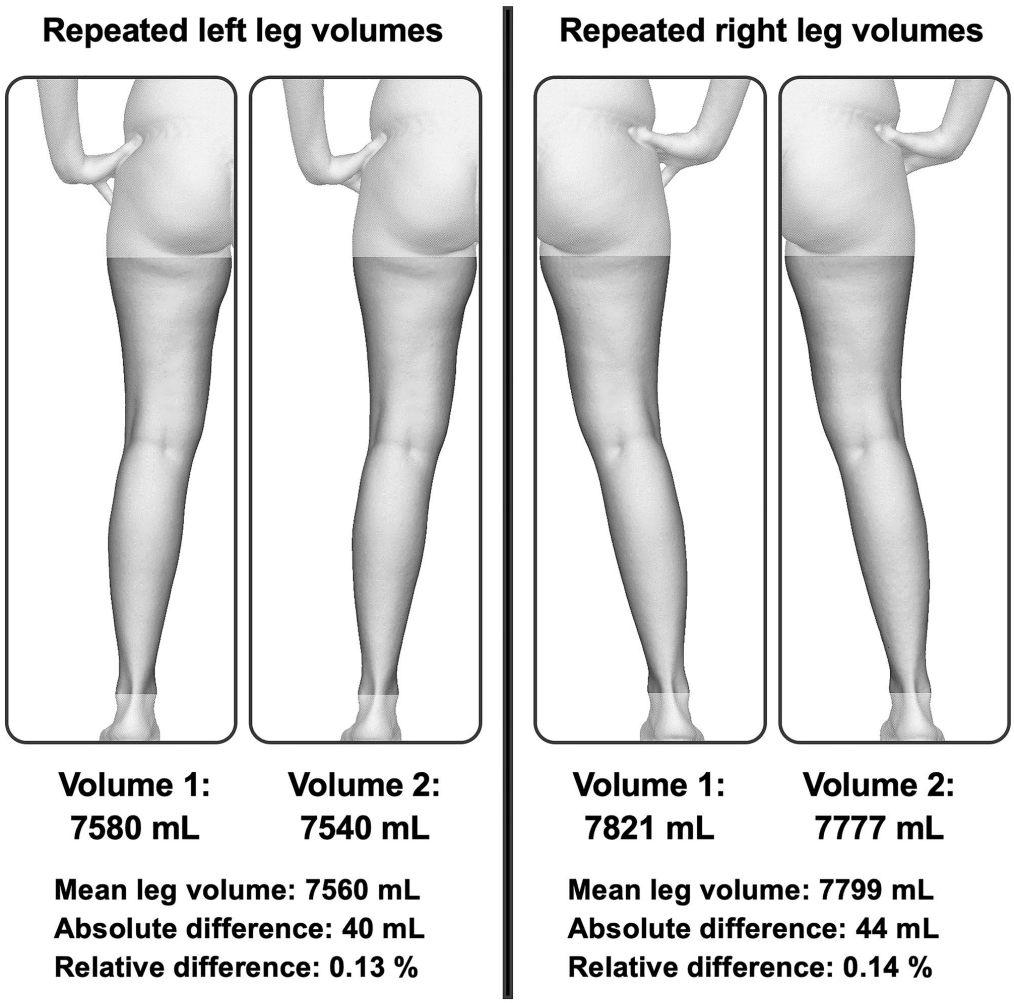

Fig. 3 Individual and mean leg volume assessment and calculation of absolute and relative differences between repeated leg scans of paired whole-body scans processed using the complete leg visibility workflow variation

Table 1 Demographic results

Cohort	Sex	Age	BMI
Entire study cohort	64 female, 18 male	41 ± 12 (21 to 71)	32.3 ± 9.7 (18.7 to 55.8)
Complete leg visibility workflow	27 female, 9 male	38 ± 13 (21 to 71)	26.4 ± 6.9 (18.7 to 44.6)
Limited leg visibility workflow	37 female, 9 male	44 ± 11 (22 to 65)	36.9 ± 9.2 (21.1 to 55.8)

All results are given as mean ± SD (standard deviation) with range in years for age and kilogram per square meter (kg/m^2) for BMI

values as well as the absolute and relative differences between repeated leg scans were calculated to gauge workflow precision. Based on the leg morphology within the 3D surface data of the subjects enrolled in this study, 36 subjects were included in the complete leg visibility workflow subgroup and 46 in the limited leg visibility workflow subgroup. A detailed overview regarding the demographic results is listed in Table 1.

Absolute Leg Volume Measurements

The average of the mean repeated leg volumes of the entire study cohort was 9752 ± 2784 mL (range 6088 to 18,970 mL) for the left side and 9841 ± 2759 mL (range 6194 to 19,690 mL) for the right side. A graphical analysis of the mean bilateral leg volume measurements in relation to the defined BMI subgroups can be seen in Fig. 4. In this graph, there are two outliers of unilateral leg volume without a corresponding value for the other leg. One is in the normal weight BMI subgroup at 12,975 mL (right leg) while the other is in the obesity class I subgroup at 16,070 mL (left leg).

A detailed overview regarding the repeated volume measurement samples as well as the mean differences and 95% confidence intervals is listed in Table 2.

When examining the entire study cohort, there was no statistically significant difference in the scores of the left leg, $t(81) = -1.143$, $p = 0.256$, and no statistically

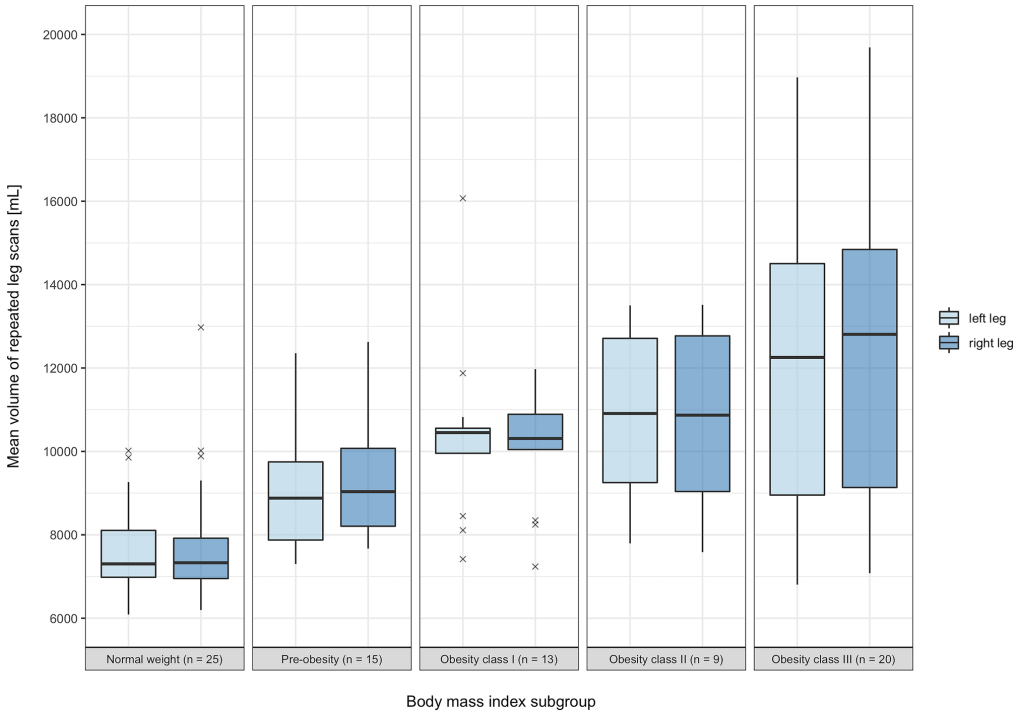

Fig. 4 Boxplot depicting the mean repeated left and right leg volume measurements in relation to the defined BMI subgroups

Table 2 Leg volume analysis of repeated whole body surface images

Cohort	Leg	Leg volume 1	Leg volume 2	Mean dif	95% CI
Entire study cohort	Left leg	9746 ± 2782	9757 ± 2787	−11.3	−30.9 to 8.3
Entire study cohort	Right leg	9845 ± 2757	9837 ± 2762	7.9	−13.1 to 28.9
Complete leg visibility workflow	Left leg	7856 ± 1148	7857 ± 1150	−0.6	−29.2 to 28.0
Complete leg visibility workflow	Right leg	8015 ± 1212	7993 ± 1227	21.8	−6.2 to 49.9
Limited leg visibility workflow	Left leg	11,225 ± 2794	11,245 ± 2792	−19.6	−47.2 to 8.0
Limited leg visibility workflow	Right leg	11,277 ± 2787	11,280 ± 2778	−3.0	−33.9 to 27.8

All results are given as mean ± SD (standard deviation) in milliliters (mL)

significant difference in the scores of the right leg, $t(81) = 0.747$, $p = 0.457$.

Furthermore, the analysis for the complete leg visibility workflow subgroup showed no statistically significant difference in the scores of the left leg, $t(35) = -0.043$, $p = 0.966$, and no statistically significant difference in the scores of the right leg, $t(35) = 1.581$, $p = 0.123$.

The assessment of the limited leg visibility workflow subgroup showed no statistically significant difference in the scores of the left leg, $t(45) = -1.433$, $p = 0.159$, and no statistically significant difference in the scores of the right leg, $t(45) = -0.199$, $p = 0.843$.

Relative Difference Between Repeated Leg Volume Measurements

The mean value of relative differences between the repeated leg volumes of the entire study cohort was 0.73 ± 0.62% (range 0.00 to 2.60%) for the left side and 0.82 ± 0.65% (range 0.00 to 3.19%) for right side. A graphical analysis of the samples of relative difference between repeated left and right leg volume measurements acquired using the complete or limited leg visibility workflow can be seen in Fig. 5.

When comparing the samples of relative difference between repeated left leg volume measurements acquired using the complete or limited leg visibility, there was no statistically significant difference in the scores; $W = 875$, $p = 0.666$. The estimated difference in location of the medians was 0.056 (95% confidence interval −0.151 to 0.328).

When comparing the samples of relative difference between repeated right leg volume measurements acquired using either the complete or the limited leg visibility workflow variation, there was no statistically significant difference in the scores, $W = 836.5$, $p = 0.940$. The estimated difference in location of the medians was 0.009 (95% confidence interval 0.268 to 0.263).

Discussion

In this study, a novel workflow for the measurement of bilateral leg volume from whole-body 3DSI was described and assessed. The data-processing procedure was specifically designed to be applicable not only when the predefined leg positioning allows full visibility of each leg, but also in cases where subject leg morphology does not allow for complete circumferential surface scan of both legs.

Following the described method, a mobile 3D imaging system consisting of a structured light scanner and an automated turntable was used for paired scans of each of the 82 subjects included in this study. As intended during study enrollment, the cohort consisted of participants with a wide BMI and leg volume range. To examine the relationship between these variables, the mean values of paired repeated leg volumes were graphically assessed dependent on the subject BMI subgroup, as is depicted in Fig. 4. While it is apparent that the subjects included in the obesity class III subgroup had the widest range of leg volume for both legs, there were some subjects with the highest BMI values who nevertheless had similarly low leg volumes to those in the normal BMI subgroup. This may be explained by the body composition of the respective subjects, as some participants had comparatively slim legs despite a bulky torso responsible for the high subject BMI value. When further examining the boxplot, it is of note that there were some outliers of mean leg volume in the normal or obesity I BMI subgroup that were only observed in one leg. The two subjects in question presenting themselves with a respective mean right leg volume of 12,975 mL and mean left leg volume of 16,070 mL were patients suffering from unilateral lymphedema. The normal BMI subgroup subject is depicted in Fig. 6. This observation positively highlights the fact that the workflow can meaningfully distinguish asymmetries, as is highly relevant for future clinical application of the presented workflow.

Because of the increasing need for objective and preferably digital forms of documentation, gathering precise data

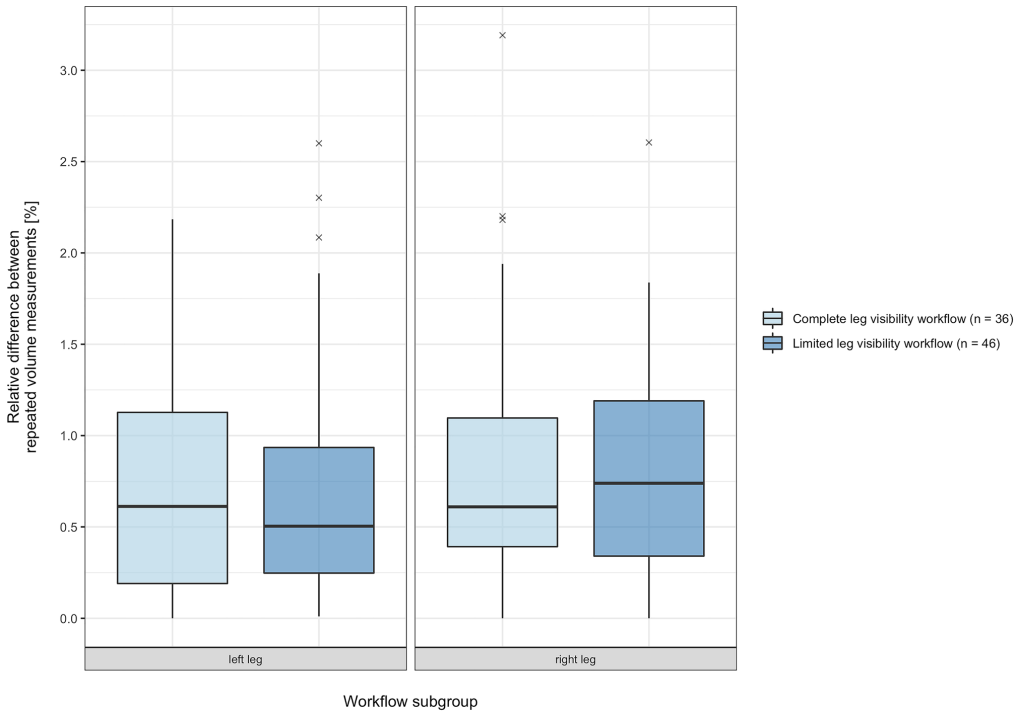

Fig. 5 Boxplot depicting the relative differences between repeated left and right leg volume measurements acquired using the complete or limited leg visibility workflow variation

regarding the human body is growing ever more important in the context of evidence based medicine. Thus, a precision assessment of a novel workflow is an essential step when the new method is intended to be applied in a clinical setting. It is therefore the subject of various 3DSI validation studies [16, 35–40]. In this study, precision was examined by bilaterally comparing the individual volume results of both repeated whole-body scans and by calculating the absolute differences as well as the relative percent difference. We found no statistically significant difference between the paired samples of absolute leg volume results. The estimated absolute differences were low, and by examining the 95 confidence intervals, these small values were further indicative that the differences in leg volume between repeated whole-body scans were of minimal clinical significance. When examining the relative percent differences to assess the deviation between repeated measures regardless of the varying individual leg volumes, we found that the mean values of both legs were below 1%. There were no values above 3.2%. When interpreting these values in a clinical context, it is important to look at the initially calculated absolute leg volumes, e.g., a 1% deviation with a mean volume of 9000 mL would result in a deviation of 90 mL. While not perfect, we deemed these absolute and relative differences between repeated scans to be negligible. We thus concluded that the workflow yielded precise results. When further comparing the relative differences of the complete and limited surface visibility cohorts, we found no statistically significant differences for either leg. We also found similarly low values for both workflow subgroups. This is depicted in Fig. 5. We therefore assumed that both worfklow variations were of similarly high precision. We thus concluded that the use of the estimation algorithm applied in the limited leg visibility workflow yields comparable results to the volume measurement conducted on completely circumferentially visible legs. We deemed these results indicative of the usefulness of standardized whole-body 3DSI as a tool to gauge changes in leg volume in clinical practice.

Nonetheless, the use of whole-body 3DSI is associated with certain drawbacks. Subjects are required to stand in an upright position with the body weight borne by both legs. This method is therefore of limited use for subjects

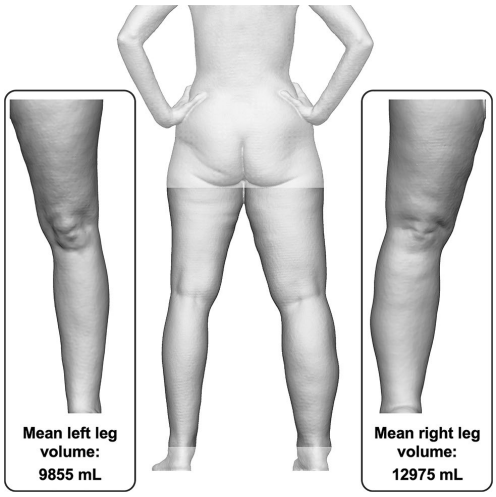

Fig. 6 Comparison of the mean left and right leg volume of a 54-year-old female subject with unilateral right-sided lymphedema whose whole-body scans were processed using the limited leg visibility workflow variation

receiving reconstructive limb surgery or in the case of limb amputation. Methods that individually assess each leg may be more useful in such cases, such as CT, MRI, or a single-leg 3DSI-based approach [12]. Also, our scanning process using a handheld scanner takes up to a minute. This requires subjects to remain standing in a fixed pose on a revolving turntable for the scan duration. In contrast, a permanently installed stereo-photogrammetric system is capable of near-instantaneous scanning. The 3DSI system presented in this study has the benefit of being a compact and portable setup and can thus allow bedside imaging. However, it may not be suitable for subjects who are prone to dizziness or with an impaired sense of balance. While the scanning duration and use of a turntable may raise the question of movement artifacts, the software used for data-processing implements a registration algorithm to align the individual scan frames. Together with the subject positioning and the instruction that patients keep their eyes open, a minimal number of movement artifacts were observed throughout the image acquisition for our study population. These artefacts were found in the upper extremity or for the head, but not for the lower extremity. We thus concluded our scanning workflow to be a robust tool for volumetric leg assessment.

A strength of this study lies in the relatively large sample size and morphologic variety of the examined subjects. While some studies assessing the precision of a workflow have examined rather small and homogenous cohorts or make use of an imaging phantom [16, 26, 39], this study included over 80 subjects in its analysis. A high number of subjects were subsequently available for each of the subgroups that were further analyzed as part of this study. Also, this study specifically examined subjects in the target population for clinical leg volume documentation. As such, it included patients with varying degrees of uni- or bilaterally high values of leg volume, and with a range of BMI values from 18.7 to 55.8 kg/m^2. While the study investigates measurement reproducibility between two separate scans in a single session, it does not provide information regarding the precision when more than two scans are conducted in one session, or when the scans are spread out over an extended period of time. Also, this study did not include multiple assessments of the same subjects by different assessors, and thus, inter-rater reliability was not examined. Future studies ought to evaluate reproducibility by repeatedly examining the same cohort without the subjects undergoing pronounced morphologic changes in the meantime. The influence of varying imaging operators should also be investigated. Finally, future efforts should be made to automate the data-processing part of the workflow.

Conclusions

The workflow presented in this study to gauge leg volume from whole-body 3D surface data was successfully applied in 82 cases. Both the standard and limited leg visibility workflow variations yielded results for leg volume quantification that were similarly precise. The workflow thus provides a precise method to digitally monitor leg volume regardless of leg morphology and could aid in objectively comparing medical treatment options of the leg in a clinical setting. Whole-body scans acquired using the described 3DSI routine may allow simultaneous assessment of other changes in body morphology after further validation.

Author Contribution LE conceived the content and conducted the 3D surface imaging, data-processing, data collection, data transformation, data analysis, figure creation, and drafted the manuscript. KCK conceived the content, assisted with subject enrollment and 3D surface imaging, and drafted the manuscript. TLS, REG, ZL and YX assisted with 3D surface imaging and aided in writing the manuscript. All authors revised the manuscript for important intellectual content and approved the final manuscript version to be submitted.

Funding Open Access funding enabled and organized by Projekt DEAL.

Declarations

Ethics Approval This study was conducted with approval from the ethics committee of the LMU Munich (reference number 17–630) and was in accordance with the 1964 Helsinki declaration and its later amendments or comparable ethical standards.

Consent to Participate Written informed consent was obtained from all individual participants included in the study.

Consent for Publication Additional written informed consent was obtained from all individual participants depicted in the the article Figures.

Conflict of Interest On behalf of all authors, the corresponding author states that there is no conflict of interest.

References

1. Kroh, A., Peters, F., Alizai, P.H., Schmitz, S., Hölzle, F., Neumann, U.P., Ulmer, F.T., Modabber, A.: 3D optical imaging as a new tool for the objective evaluation of body shape changes after bariatric surgery. Obes. Surg. 30, 1866–1873 (2020). https://doi.org/10.1007/s11695-020-04408-4
2. Ritschl, L.M., Wolff, K.D., Erben, P., Grill, F.D.: Simultaneous, radiation-free registration of the dentoalveolar position and the face by combining 3D photography with a portable scanner and impression-taking. Head Face Med. 15, 1–9 (2019). https://doi.org/10.1186/s13005-019-0212-x
3. Sutherland, J., Belec, J., Sheikh, A., Chepelev, L., Althobaity, W., Chow, B.J.W., Mitsouras, D., Christensen, A., Rybicki, F.J., La Russa, D.J.: Applying modern virtual and augmented reality technologies to medical images and models. J. Digit. Imaging. 32, 38–53 (2019). https://doi.org/10.1007/s10278-018-0122-7
4. Wilting, F.N.H., Hameeteman, M., Tielemans, H.J.P., Ulrich, D.J.O., Hummelink, S.: Three-dimensional evaluation of breast volume changes following autologous free flap breast reconstruction over six months. Breast. 50, 85–94 (2020). https://doi.org/10.1016/j.breast.2020.02.005
5. Koban, K.C., Etzel, L., Li, Z., Pazos, M., Schönecker, S., Belka, C., Giunta, R.E., Schenck, T.L., Corradini, S.: Three-dimensional surface imaging in breast cancer: a new tool for clinical studies? Radiat. Oncol. 15, 1–8 (2020). https://doi.org/10.1186/s13014-020-01499-2
6. Cotofana, S., Koban, K.C., Konstantin, F., Green, J.B., Etzel, L., Giunta, R.E., Schenck, T.L.: The surface-volume coefficient of the superficial and deep facial fat compartments: a cadaveric three-dimensional volumetric analysis. Plast. Reconstr. Surg. 143, 1605–1613 (2019). https://doi.org/10.1097/PRS.0000000000005524
7. Speir, E.J., Matthew Hawkins, C., Weiler, M.J., Briones, M., Swerdlin, R., Park, S., Brandon Dixon, J.: Volumetric assessment of pediatric vascular malformations using a rapid, hand-held three-dimensional imaging system. J. Digit. Imaging. 32, 260–268 (2019). https://doi.org/10.1007/s10278-019-00183-6
8. Cau, N., Corna, S.: Circumferential versus hand-held laser scanner method for the evaluation of lower limb volumes in normal-weight and obese subjects. J. Nov. Physiother. 6, (2016). https://doi.org/10.4172/2165-7025.1000303
9. Tokumoto, H., Akita, S., Kuriyama, M., Mitsukawa, N.: Utilization of three-dimensional photography (VECTRA) for the evaluation of lower limb lymphedema in patients following lymphovenous anastomosis. Lymphat. Res. Biol. 16, 547–552 (2018). https://doi.org/10.1089/lrb.2017.0058
10. Chromy, A., Zalud, L., Dobsak, P., Suskevic, I., Mrkvicova, V.: Limb volume measurements: comparison of accuracy and decisive parameters of the most used present methods. Springerplus. 4, (2015). https://doi.org/10.1186/s40064-015-1468-7
11. Tan, C.W., Coutts, F., Bulley, C.: Measurement of lower limb volume: agreement between the vertically oriented perometer and a tape measure method. Physiotherapy. 99, 247–251 (2013). https://doi.org/10.1016/j.physio.2012.12.004
12. Mestre, S., Veye, F., Perez-Martin, A., Behar, T., Triboulet, J., Berron, N., Demattei, C., Quéré, I.: Validation of lower limb segmental volumetry with hand-held, self-positioning three-dimensional laser scanner against water displacement. J. Vasc. Surg. Venous Lymphat. Disord. 2, 39–45 (2014). https://doi.org/10.1016/j.jvsv.2013.08.002
13. Koban, K.C., Titze, V., Etzel, L., Frank, K., Schenck, T., Giunta, R.: Quantitative volumetrische Analyse der unteren Extremität: Validierung gegenüber etablierter Maßbandmessung und Wasserverdrängung. Handchir Mikrochir Plast Chir. 50, 393–399 (2018). https://doi.org/10.1055/a-0770-3445
14. Meijer, R.S., Rietman, J.S., Geertzen, J.H., Bosmans, J.C., Dijkstra, P.U.: Validity and intra- and interobserver reliability of an indirect volume measurements in patients with upper extremity lymphedema. Lymphology. 37, 127–133 (2004)
15. Bolt, A., De Boer-Wilzing, V.G., Geertzen, J.H.B., Emmelot, C.H., Baars, E.C.T., Dijkstra, P.U.: Variation in measurements of transtibial stump model volume: a comparison of five methods. Am. J. Phys. Med. Rehabil. 89, 376–384 (2010). https://doi.org/10.1097/PHM.0b013e3181d3ea94
16. Seminati, E., Canepa Talamas, D., Young, M., Twiste, M., Dhokia, V., Bilzon, J.L.J.: Validity and reliability of a novel 3D scanner for assessment of the shape and volume of amputees' residual limb models. PLoS One. 12, e0184498 (2017). https://doi.org/10.1371/journal.pone.0184498
17. Dessery, Y., Pallari, J.: Measurements agreement between low-cost and high-level handheld 3D scanners to scan the knee for designing a 3D printed knee brace. PLoS One. 13, (2018). https://doi.org/10.1371/journal.pone.0190585
18. Lin, J.D., Chiou, W.K., Weng, H.F., Tsai, Y.H., Liu, T.H.: Comparison of three-dimensional anthropometric body surface scanning to waist-hip ratio and body mass index in correlation with metabolic risk factors. J. Clin. Epidemiol. 55, 757–766 (2002). https://doi.org/10.1016/S0895-4356(02)00433-X
19. Ng, B.K., Hinton, B.J., Fan, B., Kanaya, A.M., Shepherd, J.A.: Clinical anthropometrics and body composition from 3D whole-body surface scans. Eur. J. Clin. Nutr. Adv. online Publ. (2016). https://doi.org/10.1038/ejcn.2016.109
20. Wang, J., Gallagher, D., Thornton, J.C., Yu, W., Horlick, M., Pi-Sunyer, F.X.: Validation of a 3-dimensional photonic scanner for the measurement of body volumes, dimensions, and

percentage body fat. Am. J. Clin. Nutr. 83, 809–816 (2006). https://doi.org/10.1093/ajcn/83.4.809
21. Lu, J.M., Wang, M.J.J.: Automated anthropometric data collection using 3D whole body scanners. Expert Syst. Appl. 35, 407–414 (2008). https://doi.org/10.1016/j.eswa.2007.07.008
22. Schwarz-Müller, F., Marshall, R., Summerskill, S.: Development of a positioning aid to reduce postural variability and errors in 3D whole body scan measurements. Appl. Ergon. 68, 90–100 (2018). https://doi.org/10.1016/j.apergo.2017.11.001
23. Rapprich, S., Dingler, A., Podda, M.: Liposuction is an effective treatment for lipedema - results of a study with 25 patients. JDDG - J. Ger. Soc. Dermatology. 9, 33–40 (2011). https://doi.org/10.1111/j.1610-0387.2010.07504.x
24. Norton, J., Donaldson, N., Dekker, L.: 3D whole body scanning to determine mass properties of legs. J. Biomech. 35, 81–86 (2002). https://doi.org/10.1016/S0021-9290(01)00161-0
25. Chiu, C.Y., Pease, D.L., Fawkner, S., Sanders, R.H.: Automated body volume acquisitions from 3D structured-light scanning. Comput. Biol. Med. 101, 112–119 (2018). https://doi.org/10.1016/j.compbiomed.2018.07.016
26. Etzel, L., Koban, K.C., Li, Z., Frank, K., Giunta, R.E., Schenck, T.L.: Whole Body Surface Assessment – Implementierung und Erfahrungen von 360° 3D Ganzkörperscans: Möglichkeiten zur Objektivierung und Verlaufskontrolle an den Extremitäten und am Körperstamm. Handchir Mikrochir Plast Chir. 51, 240–248 (2019). https://doi.org/10.1055/a-0836-2683
27. R Core Team: R: a language and environment for statistical computing. (2020)
28. RStudio Team: RStudio: integrated development environment for R. (2020)
29. Rmarkdown: Dynamic documents for R. (2020)
30. Wickham, H., Averick, M., Bryan, J., Chang, W., McGowan, L.D., François, R., Grolemund, G., Hayes, A., Henry, L., Hester, J., Kuhn, M., Pedersen, T.L., Miller, E., Bache, S.M., Müller, K., Ooms, J., Robinson, D., Seidel, D.P., Spinu, V., Takahashi, K., Vaughan, D., Wilke, C., Woo, K., Yutani, H.: Welcome to the tidyverse. Journal of Open Source Software. 4, 1686 (2019). https://doi.org/10.21105/joss.01686
31. Bache, S.M., Wickham, H.: Magrittr: a forward-pipe operator for R. (2014)
32. Gohel, D.: Officer: Manipulation of Microsoft Word and Powerpoint documents. (2020)
33. Gohel, D.: Flextable: functions for tabular reporting. (2020)
34. World Health Organization: body mass index - BMI (accessed 2021–05–30), https://www.euro.who.int/en/health-topics/disease-prevention/nutrition/a-healthy-lifestyle/body-mass-index-bmi
35. Anik, A.A., Xavier, B.A., Hansmann, J., Ansong, E., Chen, J., Zhao, L., Michals, E.: Accuracy and reproducibility of linear and angular measurements in virtual reality: a validation study. J. Digit. Imaging. 33, 111–120 (2020). https://doi.org/10.1007/s10278-019-00259-3
36. Jeon, J.H., Kim, D.Y., Lee, J.J., Kim, J.H., Kim, W.C.: Repeatability and reproducibility of individual abutment impression, assessed with a blue light scanner. J. Adv. Prosthodont. 8, 214–218 (2016). https://doi.org/10.4047/jap.2016.8.3.214
37. Eder, M., Brockmann, G., Zimmermann, A., Papadopoulos, M.A., Schwenzer-Zimmerer, K., Zeilhofer, H.F., Sader, R., Papadopulos, N.A., Kovacs, L.: Evaluation of precision and accuracy assessment of different 3-D surface imaging systems for biomedical purposes. J. Digit. Imaging. 26, 163–172 (2013). https://doi.org/10.1007/s10278-012-9487-1
38. Kovacs, L., Zimmermann, A., Brockmann, G., Baurecht, H., Schwenzer-Zimmerer, K., Papadopulos, N.A., Papadopoulos, M.A., Sader, R., Biemer, E., Zeilhofer, H.F.: Accuracy and precision of the three-dimensional assessment of the facial surface using a 3-D laser scanner. IEEE Trans. Med. Imaging. 25, 742–754 (2006). https://doi.org/10.1109/TMI.2006.873624
39. Menezes, M. de, Rosati, R., Ferrario, V.F., Sforza, C.: Accuracy and reproducibility of a 3-dimensional stereophotogrammetric imaging system. J. Oral Maxillofac. Surg. 68, 2129–2135 (2010). https://doi.org/10.1016/j.joms.2009.09.036
40. Adler, C., Steinbrecher, A., Jaeschke, L., Mähler, A., Boschmann, M., Jeran, S., Pischon, T.: Validity and reliability of total body volume and relative body fat mass from a 3-dimensional photonic body surface scanner. PLoS One. 12, 1–14 (2017). https://doi.org/10.1371/journal.pone.0180201

6 Literaturverzeichnis

1. Haleem, A., Javaid, M.: 3D scanning applications in medical field: A literature-based review. Clinical Epidemiology and Global Health. 7, 199–210 (2019). https://doi.org/10.1016/j.cegh.2018.05.006

2. Tzou, C.-H.J.H.J., Frey, M.: Evolution of 3D Surface Imaging Systems in Facial Plastic Surgery. Facial Plastic Surgery Clinics of North America. 19, 591–602 (2011). https://doi.org/10.1016/j.fsc.2011.07.003

3. Tzou, C.H.J., Artner, N.M., Pona, I., Hold, A., Placheta, E., Kropatsch, W.G., Frey, M.: Comparison of three-dimensional surface-imaging systems. Journal of Plastic, Reconstructive and Aesthetic Surgery. 67, 489–497 (2014). https://doi.org/10.1016/j.bjps.2014.01.003

4. Chang, J.B., Small, K.H., Choi, M., Karp, N.S.: Three-Dimensional Surface Imaging in Plastic Surgery: Foundation, Practical Applications, and beyond. Plastic and Reconstructive Surgery. 135, 1295–1304 (2015). https://doi.org/10.1097/PRS.0000000000001221

5. Li, Y., Yang, X., Li, D.: The application of three-dimensional surface imaging system in plastic and reconstructive surgery. Annals of Plastic Surgery. 77, S76–S83 (2016). https://doi.org/10.1097/SAP.0000000000000813

6. Xu, Y., Frank, K., Kohler, L., Ehrl, D., Alfertshofer, M., Giunta, R.E., Moellhoff, N., Cotofana, S., Koban, K.C.: Reliability of 3-dimensional surface imaging of the face using a whole-body surface scanner. Journal of Cosmetic Dermatology. 21, 1464–1470 (2022). https://doi.org/10.1111/jocd.14555

7. Koban, K.C., Perko, P., Etzel, L., Li, Z., Schenck, T.L., Giunta, R.E.: Validation of two handheld devices against a non-portable three-dimensional surface scanner and assessment of potential use for intraoperative facial imaging. Journal of Plastic, Reconstructive and Aesthetic Surgery. 73, 141–148 (2020). https://doi.org/10.1016/j.bjps.2019.07.008

8. Koban, K.C., Frank, K., Etzel, L., Schenck, T.L., Giunta, R.E.: 3D Mammometric Changes in the Treatment of Idiopathic Gynecomastia. Aesthetic Plastic Surgery. 43, 616–624 (2019). https://doi.org/10.1007/s00266-019-01341-5

9. Metzler, P., Sun, Y., Zemann, W., Bartella, A., Lehner, M., Obwegeser, J.A. nton, Kruse-Gujer, A.L., Lübbers, H.T.: Validity of the 3D VECTRA photogrammetric surface imaging system for cranio-maxillofacial anthropometric measurements. Oral and maxillofacial surgery. 18, 297–304 (2014). https://doi.org/10.1007/s10006-013-0404-7

10. Jodeh, D.S., Rottgers, S.A.: High-Fidelity Anthropometric Facial Measurements Can Be Obtained From a Single Stereophotograph From the Vectra H1 3-Dimensional Camera. Cleft Palate-Craniofacial Journal. 56, 1164–1170 (2019). https://doi.org/10.1177/1055665619839577

11. Liu, C., Artopoulos, A.: Validation of a low-cost portable 3-dimensional face scanner. Imaging Science in Dentistry. 49, 35–43 (2019). https://doi.org/10.5624/isd.2019.49.1.35

12. Gibelli, D., Pucciarelli, V., Cappella, A., Dolci, C., Sforza, C.: Are Portable Stereophotogrammetric Devices Reliable in Facial Imaging? A Validation Study of VECTRA H1 Device. Journal of Oral and Maxillofacial Surgery. 76, 1772–1784 (2018). https://doi.org/10.1016/j.joms.2018.01.021

13. Tong, O.L.H., Chamson-Reig, A., Yip, L.C.M., Brackstone, M., Diop, M., Carson, J.J.L.: Structured-light surface scanning system to evaluate breast morphology in standing and supine positions. Scientific Reports. 10, 14087 (2020). https://doi.org/10.1038/s41598-020-70476-2

14. Etzel, L., Koban, K.C., Li, Z., Frank, K., Giunta, R.E., Schenck, T.L.: Whole-body surface assessment - Implementation and experiences with 360° 3D whole-body scans: Opportunities to objectively monitor the extremities and the body trunk. Handchirurgie Mikrochirurgie Plastische Chirurgie. 51, 240–248 (2019). https://doi.org/10.1055/a-0836-2683

15. Modabber, A., Peters, F., Kniha, K., Goloborodko, E., Ghassemi, A., Lethaus, B., Hölzle, F., Möhlhenrich, S.C.: Evaluation of the accuracy of a mobile and a stationary system for three-dimensional facial scanning. Journal of Cranio-Maxillofacial Surgery. 44, 1719–1724 (2016). https://doi.org/10.1016/j.jcms.2016.08.008

16. Epstein, M.D., Scheflan, M.: Three-dimensional Imaging and Simulation in Breast Augmentation. What Is the Current State of the Art? Clinics in Plastic Surgery. 42, 437–450 (2015). https://doi.org/10.1016/j.cps.2015.06.013

17. Tsay, C., Zhu, V., Sturrock, T., Shah, A., Kwei, S.: A 3D Mammometric Comparison of Implant-Based Breast Reconstruction With and Without Acellular Dermal Matrix (ADM). Aesthetic Plastic Surgery. 42, 49–58 (2018). https://doi.org/10.1007/s00266-017-0967-z

18. Tepper, O.M., Small, K.H., Unger, J.G., Feldman, D.L., Kumar, N., Choi, M., Karp, N.S.: 3D Analysis of Breast Augmentation Defines Operative Changes and Their Relationship to Implant Dimensions. Annals of Plastic Surgery. 62, 570–575 (2009). https://doi.org/10.1097/SAP.0b013e31819faff9

19. Eder, M., Waldenfels, F.v., Swobodnik, A., Klöppel, M., Pape, A.K., Schuster, T., Raith, S., Kitzler, E., Papadopulos, N.A., Machens, H.G., Kovacs, L.: Objective breast symmetry evaluation using 3-D surface imaging. Breast. 21, 152–158 (2012). https://doi.org/10.1016/j.breast.2011.07.016

20. Coltman, C.E., McGhee, D.E., Steele, J.R.: Three-dimensional scanning in women with large, ptotic breasts: implications for bra cup sizing and design. Ergonomics. 60, 439–445 (2017). https://doi.org/10.1080/00140139.2016.1176258

21. Donfrancesco, A., Montemurro, P., Hedén, P.: Three-dimensional simulated images in breast augmentation surgery: An investigation of patients' satisfaction and the correlation between prediction and actual outcome. Plastic and Reconstructive Surgery. 132, 810–822 (2013). https://doi.org/10.1097/PRS.0b013e3182a014cb

22. Koban, K.C., Schenck, T., Metz, P.M., Volkmer, E., Haertnagl, F., Titze, V., Giunta, R.E.: Auf dem Weg zur objektiven Evaluation von Form, Volumen und Symmetrie in der Plastischen Chirurgie mittels intraoperativer 3D Scans. Handchirurgie Mikrochirurgie Plastische Chirurgie. 48, 78–84 (2016). https://doi.org/10.1055/s-0042-104506

23. Roostaeian, J., Adams, W.P.: Three-dimensional imaging for breast augmentation: Is this technology providing accurate simulations? Aesthetic Surgery Journal. 34, 857–875 (2014). https://doi.org/10.1177/1090820X14538805

24. Kroh, A., Peters, F., Alizai, P.H., Schmitz, S., Hölzle, F., Neumann, U.P., Ulmer, F.T., Modabber, A.: 3D Optical Imaging as a New Tool for the Objective Evaluation of Body Shape Changes After Bariatric Surgery. Obesity Surgery. 30, 1866–1873 (2020). https://doi.org/10.1007/s11695-020-04408-4

25. Speir, E.J., Matthew Hawkins, C., Weiler, M.J., Briones, M., Swerdlin, R., Park, S., Brandon Dixon, J.: Volumetric Assessment of Pediatric Vascular Malformations Using a Rapid, Hand-Held Three-Dimensional Imaging System. Journal of Digital Imaging. 32, 260–268 (2019). https://doi.org/10.1007/s10278-019-00183-6

26. Ritschl, L.M., Wolff, K.D., Erben, P., Grill, F.D.: Simultaneous, radiation-free registration of the dentoalveolar position and the face by combining 3D photography with a portable scanner and impression-taking. Head and Face Medicine. 15, 1–9 (2019). https://doi.org/10.1186/s13005-019-0212-x

27. Seminati, E., Canepa Talamas, D., Young, M., Twiste, M., Dhokia, V., Bilzon, J.L.J.: Validity and reliability of a novel 3D scanner for assessment of the shape and volume of amputees' residual limb models. PLOS ONE. 12, e0184498 (2017). https://doi.org/10.1371/journal.pone.0184498

28. Bulstrode, N., Bellamy, E., Shrotria, S.: Breast volume assessment: Comparing five different techniques. Breast. 10, 117–123 (2001). https://doi.org/10.1054/brst.2000.0196

29. Cotofana, S., Koban, K.C., Konstantin, F., Green, J.B., Etzel, L., Giunta, R.E., Schenck, T.L.: The Surface-Volume Coefficient of the Superficial and Deep Facial Fat Compartments: A Cadaveric Three-Dimensional Volumetric Analysis. Plastic and Reconstructive Surgery. 143, 1605–1613 (2019). https://doi.org/10.1097/PRS.0000000000005524

30. Koban, K.C., Titze, V., Etzel, L., Frank, K., Schenck, T., Giunta, R.: Quantitative volumetric analysis of the lower extremity: Validation against established tape measurement and water displacement. Handchirurgie Mikrochirurgie Plastische Chirurgie. 50, 393–399 (2018). https://doi.org/10.1055/a-0770-3445

31. Koban, K.C., Cotofana, S., Frank, K., Green, J.B., Etzel, L., Li, Z., Giunta, R.E., Schenck, T.L.: Precision in 3-Dimensional Surface Imaging of the Face: A Handheld Scanner Comparison Performed in a Cadaveric Model. Aesthetic Surgery Journal. 39, NP36–NP44 (2019). https://doi.org/10.1093/asj/sjy242

32. Modabber, A., Peters, F., Brokmeier, A., Goloborodko, E., Ghassemi, A., Lethaus, B., Hölzle, F., Möhlhenrich, S.C., SURNAME, N.: Influence of Connecting Two Standalone Mobile Three-Dimensional Scanners on Accuracy Comparing with a Standard Device in Facial Scanning. Journal of Oral and Maxillofacial Research. 7, e4 (2016). https://doi.org/10.5037/jomr.2016.7404

33. Grant, C.A., Johnston, M., Adam, C.J., Little, J.P.: Accuracy of 3D surface scanners for clinical torso and spinal deformity assessment. Medical Engineering and Physics. 63, 63–71 (2019). https://doi.org/10.1016/j.medengphy.2018.11.004

34. Yamamoto, S., Miyachi, H., Fujii, H., Ochiai, S., Watanabe, S., Shimozato, K.: Intuitive Facial Imaging Method for Evaluation of Postoperative Swelling: A Combination of 3-Dimensional Computed Tomography and Laser Surface Scanning in Orthognathic Surgery. Journal of Oral and Maxillofacial Surgery. 74, 2506.e1–2506.e10 (2016). https://doi.org/10.1016/j.joms.2016.08.039

35. Schenck, T.L., Koban, K.C., Schlattau, A., Frank, K., Sclafani, A.P., Giunta, R.E., Roth, M.Z., Gaggl, A., Gotkin, R.H., Cotofana, S.: Updated anatomy of the buccal space and its implications for plastic, reconstructive and aesthetic procedures. Journal of Plastic, Reconstructive and Aesthetic Surgery. 71, 162–170 (2018). https://doi.org/10.1016/j.bjps.2017.11.005

36. Wilting, F.N.H.H., Hameeteman, M., Tielemans, H.J.P.P., Ulrich, D.J.O.O., Hummelink, S.: “Three-dimensional evaluation of breast volume changes following autologous free flap breast

reconstruction over six months". Breast. 50, 85–94 (2020). https://doi.org/10.1016/j.breast.2020.02.005

37. Reitz, D., Carl, G., Schönecker, S., Pazos, M., Freislederer, P., Niyazi, M., Ganswindt, U., Alongi, F., Reiner, M., Belka, C., Corradini, S.: Real-time intra-fraction motion management in breast cancer radiotherapy: Analysis of 2028 treatment sessions. Radiation Oncology. 13, 128 (2018). https://doi.org/10.1186/s13014-018-1072-4

38. Carl, G., Reitz, D., Schönecker, S., Pazos, M., Freislederer, P., Reiner, M., Alongi, F., Niyazi, M., Ganswindt, U., Belka, C., Corradini, S.: Optical surface scanning for patient positioning in radiation therapy: A prospective analysis of 1902 fractions. Technology in Cancer Research and Treatment. 17, 153303381880600 (2018). https://doi.org/10.1177/1533033818806002

39. Schonecker, S., Walter, F., Freislederer, P., Marisch, C., Scheithauer, H., Harbeck, N., Corradini, S., Belka, C.: Treatment planning and evaluation of gated radiotherapy in left-sided breast cancer patients using the CatalystTM/SentinelTM system for deep inspiration breath-hold (DIBH). Radiation Oncology. 11, 1–10 (2016). https://doi.org/10.1186/s13014-016-0716-5

40. Hamming, V.C., Visser, C., Batin, E., McDermott, L.N., Busz, D.M., Both, S., Langendijk, J.A., Sijtsema, N.M.: Evaluation of a 3D surface imaging system for deep inspiration breath-hold patient positioning and intra-fraction monitoring. Radiation Oncology. 14, 125 (2019). https://doi.org/10.1186/s13014-019-1329-6

41. Borm, K.J., Loos, M., Oechsner, M., Mayinger, M.C., Paepke, D., Kiechle, M.B., Combs, S.E., Duma, M.N.: Acute radiodermatitis in modern adjuvant 3D conformal radiotherapy for breast cancer - the impact of dose distribution and patient related factors. Radiation Oncology. 13, 218 (2018). https://doi.org/10.1186/s13014-018-1160-5

42. Liang, X., Bradley, J.A., Zheng, D., Rutenberg, M., Yeung, D., Mendenhall, N., Li, Z.: Prognostic factors of radiation dermatitis following passive-scattering proton therapy for breast cancer. Radiation Oncology. 13, 72 (2018). https://doi.org/10.1186/s13014-018-1004-3

43. Partl, R., Lehner, J., Winkler, P., Kapp, K.S.: Testing the feasibility of augmented digital skin imaging to objectively compare the efficacy of topical treatments for radiodermatitis. PLoS ONE. 14, 1–11 (2019). https://doi.org/10.1371/journal.pone.0218018

44. Partl, R., Jonko, B., Schnidar, S., Schollhammer, M., Bauer, M., Singh, S., Simeckova, J., Wiesner, K., Neubauer, A., Schnidar, H.: 128 SHADES of RED: Objective remote assessment of radiation dermatitis by augmented digital skin imaging. In: Studies in health technology and informatics. pp. 363–374. IOS Press (2017)

45. Lu, J.M., Wang, M.J.J.: Automated anthropometric data collection using 3D whole body scanners. Expert Systems with Applications. 35, 407–414 (2008). https://doi.org/10.1016/j.eswa.2007.07.008

46. Lin, J.D., Chiou, W.K., Weng, H.F., Tsai, Y.H., Liu, T.H.: Comparison of three-dimensional anthropometric body surface scanning to waist-hip ratio and body mass index in correlation with metabolic risk factors. Journal of Clinical Epidemiology. 55, 757–766 (2002). https://doi.org/10.1016/S0895-4356(02)00433-X

47. Xu, Y., Frank, K., Kohler, L., Ehrl, D., Alfertshofer, M., Giunta, R.E., Moellhoff, N., Cotofana, S., Koban, K.C.: Reliability of 3-dimensional surface imaging of the face using a whole-body surface scanner. Journal of Cosmetic Dermatology. 1–7 (2021). https://doi.org/10.1111/jocd.14555

48. Schwarz-Müller, F., Marshall, R., Summerskill, S.: Development of a positioning aid to reduce postural variability and errors in 3D whole body scan measurements. Applied Ergonomics. 68, 90–100 (2018). https://doi.org/10.1016/j.apergo.2017.11.001

49. Adler, C., Steinbrecher, A., Jaeschke, L., Mähler, A., Boschmann, M., Jeran, S., Pischon, T.: Validity and reliability of total body volume and relative body fat mass from a 3-dimensional photonic body surface scanner. PLoS ONE. 12, 1–14 (2017). https://doi.org/10.1371/journal.pone.0180201

50. Ng, B.K., Hinton, B.J., Fan, B., Kanaya, A.M., Shepherd, J.A.: Clinical anthropometrics and body composition from 3D whole-body surface scans. European Journal of Clinical Nutrition advance online publication. (2016). https://doi.org/10.1038/ejcn.2016.109

51. Wang, J., Gallagher, D., Thornton, J.C., Yu, W., Horlick, M., Pi-Sunyer, F.X.: Validation of a 3-dimensional photonic scanner for the measurement of body volumes, dimensions, and percentage body fat. American Journal of Clinical Nutrition. 83, 809–816 (2006). https://doi.org/10.1093/ajcn/83.4.809

52. Chiu, C.Y., Pease, D.L., Fawkner, S., Sanders, R.H.: Automated body volume acquisitions from 3D structured-light scanning. Computers in Biology and Medicine. 101, 112–119 (2018). https://doi.org/10.1016/j.compbiomed.2018.07.016

53. Bolt, A., De Boer-Wilzing, V.G., Geertzen, J.H.B.B., Emmelot, C.H., Baars, E.C.T.T., Dijkstra, P.U.: Variation in measurements of transtibial stump model volume: A comparison of five methods. American Journal of Physical Medicine and Rehabilitation. 89, 376–384 (2010). https://doi.org/10.1097/PHM.0b013e3181d3ea94

54. Cau, N., Corna, S.: Circumferential versus Hand-held Laser Scanner Method for the Evaluation of Lower Limb Volumes in Normal-weight and Obese Subjects. Journal of Novel Physiotherapies. 6, (2016). https://doi.org/10.4172/2165-7025.1000303

55. Norton, J., Donaldson, N., Dekker, L.: 3D whole body scanning to determine mass properties of legs. Journal of Biomechanics. 35, 81–86 (2002). https://doi.org/10.1016/S0021-9290(01)00161-0

56. Rapprich, S., Dingler, A., Podda, M.: Liposuction is an effective treatment for lipedema - Results of a study with 25 patients. JDDG - Journal of the German Society of Dermatology. 9, 33–40 (2011). https://doi.org/10.1111/j.1610-0387.2010.07504.x

57. Chromy, A., Zalud, L., Dobsak, P., Suskevic, I., Mrkvicova, V.: Limb volume measurements: comparison of accuracy and decisive parameters of the most used present methods. SpringerPlus. 4, (2015). https://doi.org/10.1186/s40064-015-1468-7

58. Dessery, Y., Pallari, J.: Measurements agreement between low-cost and high-level handheld 3D scanners to scan the knee for designing a 3D printed knee brace. PLoS ONE. 13, (2018). https://doi.org/10.1371/journal.pone.0190585

59. Tokumoto, H., Akita, S., Kuriyama, M., Mitsukawa, N.: Utilization of Three-Dimensional Photography (VECTRA) for the Evaluation of Lower Limb Lymphedema in Patients Following Lymphovenous Anastomosis. Lymphatic Research and Biology. 16, 547–552 (2018). https://doi.org/10.1089/lrb.2017.0058

60. Mestre, S., Veye, F., Perez-Martin, A., Behar, T., Triboulet, J., Berron, N., Dematteï, C., Quéré, I.: Validation of lower limb segmental volumetry with hand-held, self-positioning three-

dimensional laser scanner against water displacement. Journal of Vascular Surgery: Venous and Lymphatic Disorders. 2, 39–45 (2014). https://doi.org/10.1016/j.jvsv.2013.08.002

61. Tan, C.-W., Coutts, F., Bulley, C.: Measurement of lower limb volume: Agreement between the vertically oriented perometer and a tape measure method. Physiotherapy. 99, 247–251 (2013). https://doi.org/10.1016/j.physio.2012.12.004

62. Jeon, J.H., Kim, D.Y., Lee, J.J., Kim, J.H., Kim, W.C.: Repeatability and reproducibility of individual abutment impression, assessed with a blue light scanner. Journal of Advanced Prosthodontics. 8, 214–218 (2016). https://doi.org/10.4047/jap.2016.8.3.214

63. Kovacs, L., Zimmermann, A., Brockmann, G., Baurecht, H., Schwenzer-Zimmerer, K., Papadopulos, N.A., Papadopoulos, M.A., Sader, R., Biemer, E., Zeilhofer, H.F.: Accuracy and precision of the three-dimensional assessment of the facial surface using a 3-D laser scanner. IEEE Transactions on Medical Imaging. 25, 742–754 (2006). https://doi.org/10.1109/TMI.2006.873624

64. Anik, A.A., Xavier, B.A., Hansmann, J., Ansong, E., Chen, J., Zhao, L., Michals, E.: Accuracy and Reproducibility of Linear and Angular Measurements in Virtual Reality: a Validation Study. Journal of Digital Imaging. 33, 111–120 (2020). https://doi.org/10.1007/s10278-019-00259-3

65. Hopwood, P., Haviland, J.S., Sumo, G., Mills, J., Bliss, J.M., Yarnold, J.R.: Comparison of patient-reported breast, arm, and shoulder symptoms and body image after radiotherapy for early breast cancer: 5-year follow-up in the randomised Standardisation of Breast Radiotherapy (START) trials. The Lancet Oncology. 11, 231–240 (2010). https://doi.org/10.1016/S1470-2045(09)70382-1

66. Shaitelman, S.F., Lei, X., Thompson, A., Schlembach, P., Bloom, E.S., Arzu, I.Y., Buchholz, D., Chronowski, G., Dvorak, T., Grade, E., Hoffman, K., Perkins, G., Reed, V.K., Shah, S.J., Stauder, M.C., Strom, E.A., Tereffe, W., Woodward, W.A., Amaya, D.N., Shen, Y., Hortobagyi, G.N., Hunt, K.K., Buchholz, T.A., Smith, B.D.: Three-Year Outcomes With Hypofractionated Versus Conventionally Fractionated Whole-Breast Irradiation: Results of a Randomized, Noninferiority Clinical Trial. Journal of Clinical Oncology. 36, 3495–3503 (2018). https://doi.org/10.1200/JCO.18.00317

67. Agrawal, R.K., Aird, E.G.A., Barrett, J.M., Barrett-Lee, P.J., Bentzen, S.M., Bliss, J.M., Brown, J., Dewar, J.A., Dobbs, H.J., Haviland, J.S., Hoskin, P.J., Hopwood, P., Lawton, P.A., Magee, B.J., Mills, J., Morgan, D.A.L., Owen, J.R., Simmons, S., Sumo, G., Sydenham, M.A., Venables, K., Yarnold, J.R., Daly, M., Moody, A.M., Patterson, H., Singer, J., Williams, M.V., Wilson, C.B., Magee, B.J., Stewart, A., Sykes, A., Errington, D., Myint, S., Syndikus, I., Thorp, N., Dyson, P., Nicoll, J.J., Kelly, S., Dobbs, J., Harris, S., MacDonald, E.A., O'Connell, M., Timothy, A.R., LeVay, J., Hardman, P.D.J., Storey, N., Wadd, N., Khanna, S., Madden, F., Osmond, A., Peat, I., Abson, C., Dubois, J.D., McKinna, F., Pickering, D., Sadler, G., Ashford, R., Grosch, E., Harrison, M., Maher, E.J., Makris, A., Ostler, P., Allerton, R., Brammer, C., Churn, M., Fairlamb, D., Priestman, T., Bulman, A.S., Martin, W.M.C., Gibbs, Money-Kyrle, J., Quigley, M., Bliss, P., Goodman, A.G., Hong, A., Rowland, Biswas, A., Kumar, S., Reed, G., Skailes, G.E., Golding, P.F., Khoury, G.G., Low, E., Robinson, A., Trask, C., Bloomfield, D., Deutsch, G.P., Hodson, N., Goodman, A.G., Brunt, A.M., Cook, J., Dunn, K., Hatton, M., Purohit, O., Ramakrishnan, S., Robinson, M., Barrett, A., Armitage, M., Chetty, U., Mayles, P., Walker, L., Lucraft, H., Parmar, M., Turesson, I., Carling, M., Pritchard, J., King, M., Parkin, E., Law, K., Perkins, S., Wells, U., Yarnold, J.R.: The UK Standardisation of Breast Radiotherapy (START)

Trial B of radiotherapy hypofractionation for treatment of early breast cancer: a randomised trial. The Lancet. 371, 1098–1107 (2008). https://doi.org/10.1016/S0140-6736(08)60348-7

Danksagung

An erster Stelle bedanke ich mich herzlich bei meinem Doktorvater Herrn Univ.-Professor Dr. Giunta für die Bereitstellung des Themas, für die Betreuung und das mir entgegengebrachte Vertrauen sowie für die Möglichkeit zum selbstständigen wissenschaftlichen Arbeiten.

Ein großer Dank gilt Herrn Professor Dr. Schenck für die Mitbetreuung und Lehre während meiner wissenschaftlichen und klinischen Tätigkeit als Doktorand.

Weiter spreche ich allen Patientinnen und Probanden meinen Dank aus, die diese Arbeit mit ihrer Teilnahme an den vorliegenden Publikationen ermöglicht haben.

Ich danke dem gesamten Team der Abteilung für Hand-, Plastische und Ästhetische Chirurgie am LMU Klinikum für die Unterstützung und Lehre im wissenschaftlichen und klinischen Alltag.

Dem Team der Klinik und Poliklinik für Strahlentherapie und Radioonkologie am LMU Klinikum möchte ich herzlich für die interdisziplinäre Kooperation und für die Einblicke in das Fach der Radioonkologie danken.

Ein ganz besonderer Dank gilt Herrn Dr. Koban für die stets entgegenbrachte Motivation und Freude an der Zusammenarbeit, für den fortwährenden intellektuellen und freundschaftlichen Austausch innerhalb und außerhalb der Klinik, sowie für die wiederholte Versorgung mit koffeinhaltigen Kaltgetränken.

Schließlich bedanke ich mich ganz herzlich bei meiner Familie und meinen Freunden für deren andauernden Rückhalt und die konstante Unterstützung.